AD-A061 608 ARMY ELECTRONICS RESEARCH AND DEVELOPMENT COMMAND WS--ETC F/G 7/4
PRESSURE DEPENDENCE OF THE WATER VAPOR CONTINUUM ABSORPTION IN --ETC(U)
SEP 78 W R WATKINS, K O WHITE, L R BOWER

UNCLASSIFIED ERADCOM-ASL-TR-0017 NL

1 OF 1
AD
A061 608

END
DATE
FILMED
2-79
DDC

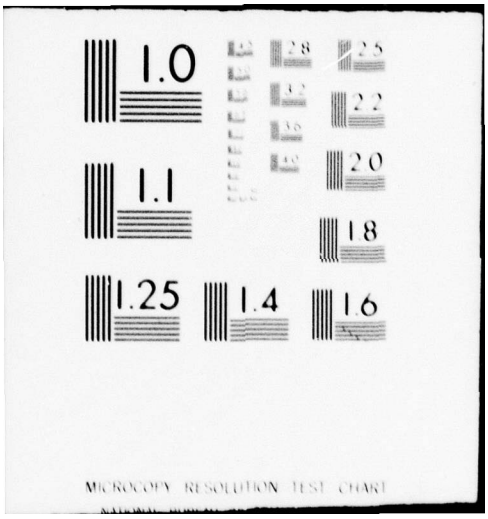
1.0
1.1
1.25
1.4
1.6
2.8
3.2
3.6
4.0
2.5
2.2
2.0
1.8
MICROCOPY RESOLUTION TEST CHART

ERADCOM-
ASL-TR-0017

AD
Reports Control Symbol
OSD-1366

LEVEL II

PRESSURE DEPENDENCE OF THE WATER VAPOR CONTINUUM ABSORPTION IN THE 3.5 TO 4.0 MICROMETER REGION

Technical rept.,

SEPT[illegible]78

44p.

By

WENDELL R. WATKINS,
KENNETH O. WHITE,
LANNY B. BOWER
BRIAN Z. SOJKA

1L161102B53A

Approved for public release; distribution unlimited

US Army Electronics Research and Development Command
Atmospheric Sciences Laboratory
White Sands Missile Range, NM 88002

NOTICES

Disclaimers

The findings in this report are not to be construed as an official Department of the Army position, unless so designated by other authorized documents.

The citation of trade names and names of manufacturers in this report is not to be construed as official Government indorsement or approval of commercial products or services referenced herein.

Disposition

Destroy this report when it is no longer needed. Do not return it to the originator.

SECURITY CLASSIFICATION OF THIS PAGE *(When Data Entered)*

REPORT DOCUMENTATION PAGE

READ INSTRUCTIONS BEFORE COMPLETING FORM

1. REPORT NUMBER: ASL-TR-0017	2. GOVT ACCESSION NO.
3. RECIPIENT'S CATALOG NUMBER	
4. TITLE *(and Subtitle)*: PRESSURE DEPENDENCE OF THE WATER VAPOR CONTINUUM ABSORPTION IN THE 3.5- TO 4.0-MICROMETER REGION	5. TYPE OF REPORT & PERIOD COVERED: R&D Technical Report
	6. PERFORMING ORG. REPORT NUMBER
7. AUTHOR(s): Wendell R. Watkins, Lanny R. Bower, Kenneth O. White, Brian Z. Sojka	8. CONTRACT OR GRANT NUMBER(s)
9. PERFORMING ORGANIZATION NAME AND ADDRESS: Atmospheric Sciences Laboratory, White Sands Missile Range, New Mexico 88002	10. PROGRAM ELEMENT, PROJECT, TASK AREA & WORK UNIT NUMBERS: DA Task No. 1L161102B53A
11. CONTROLLING OFFICE NAME AND ADDRESS: US Army Electronics Research and Development Command, Adelphi, MD 20783	12. REPORT DATE: SEPTEMBER 1978
	13. NUMBER OF PAGES: 39
14. MONITORING AGENCY NAME & ADDRESS *(if different from Controlling Office)*	15. SECURITY CLASS. *(of this report)*: UNCLASSIFIED
	15a. DECLASSIFICATION/DOWNGRADING SCHEDULE

16. DISTRIBUTION STATEMENT *(of this Report)*

Approved for public release; distribution unlimited.

17. DISTRIBUTION STATEMENT *(of the abstract entered in Block 20, if different from Report)*

18. SUPPLEMENTARY NOTES

19. KEY WORDS *(Continue on reverse side if necessary and identify by block number)*

Absorption	Lasers
Pressure dependence	Spectroscopy
Atmospheric optics	Water vapor
Infrared	Continuum Model

20. ABSTRACT *(Continue on reverse side if necessary and identify by block number)*

Measurements of water vapor continuum absorption in the 3.5- to 4.0-micrometer region are presented. A deuterium fluoride grating tunable laser was used in conjunction with a 21-m long-path absorption cell. Measurements were performed at 25°C with 14.3 torr of deuterium depleted water vapor (one-fiftieth the normal concentration of HDO) buffered by pressures of 0, 250, 500, 750, 1000, and 1250 torr of an 80/20 mixture of N_2/O_2. From the measurements of the water vapor continuum absorption

DD FORM 1 JAN 73 1473 EDITION OF 1 NOV 65 IS OBSOLETE

SECURITY CLASSIFICATION OF THIS PAGE *(When Data Entered)*

20. ABSTRACT (cont)

at 26 laser lines for the six foreign broadening pressures, a foreign-to-self-broadening coefficient of 0.011 with a factor of 2 uncertainty was obtained. This coefficient is an order of magnitude smaller than the value of 0.12 measured (under higher temperature and pressure conditions) by other workers. Strength values for the water vapor continuum for 14.3 torr of water vapor buffered to 760 torr total pressure by an 80/20 mixture of N_2/O_2 at 23°C previously measured in this laboratory were further substantiated by these measurements. A new model was developed for the water vapor continuum comprised of both far wing and aggregate-water-molecule type contributions. The previous 23°C data and the new 25°C data were used to calculate the water vapor continuum absorption in the 3.5- to 4.0-micrometer spectral region as a function of relative humidity for standard atmospheric pressure and ambient temperatures. Updating the presently used data base for this spectral region with these new values will have significant impact on the accuracy of the modeling of atmospheric transmission effects for Army electro-optical systems. In particular the results of this study show that the partial pressure of water vapor, especially at low total pressures, is more important than previously anticipated.

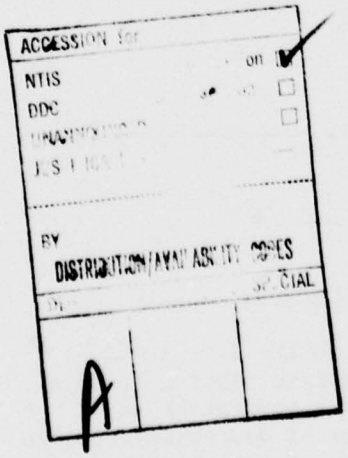

CONTENTS

SUMMARY

This report contains the first ambient temperature measurements of the pressure dependence of the water vapor continuum absorption in the 3.5- to 4.0-micrometer spectral region. In particular, an extensive set of measurements at 25°C has resulted in a measured value of the foreign-to-self-broadening coefficient of 0.011. This value was found to be frequency dependent and is an order of magnitude smaller than the value of 0.12 measured by Burch et al. at higher temperatures. This self-contribution to the water vapor continuum was nearly an order of magnitude larger than predicted by the Burch extrapolation scheme based on his higher temperature measurements. These results were used to formulate a new model for the water vapor continuum in the 3- to 5-micrometer window. The continuum appears to have contributions from both far wing type and aggregate-water-molecule type absorption, the latter having little or no foreign broadening dependence. Calculations are presented for the absorption due to the water vapor continuum as a function of relative humidity at ambient temperature and standard pressure using the new model based on the new 25°C data and previous measurements at 23°C. The temperature dependence of this model will soon be determined by measurements in progress at the Atmospheric Sciences Laboratory (ASL) and will be reported at a later date.

The results presented in this report will increase the accuracy of modeling results used for the performance prediction and evaluation of Army and DoD electro-optical and high energy laser systems.

PREFACE

The authors thank Robert L. Spellicy for his critical review of the manuscript.

INTRODUCTION

An accurate and detailed knowledge of atmospheric transmission in and near the infrared spectral windows is essential to the design, performance evaluation, and comparative testing of electro-optical (EO) systems [1]. Of the many contributors to gaseous absorption in the atmosphere, water vapor is the most widespread spectrally and of greatest concern for many practical applications, especially for long-path high-visibility conditions. A major stumbling block to obtaining usable modeling predictions for Army EO including high energy laser (HEL) systems is lack of an accurate data base for the water vapor continuum absorption in the 3- to 5-micrometer window. Although recent measurements by the ASL have significantly improved the strength predictions for this continuum under ambient temperature and pressure conditions [1], the parameters needed to describe temperature and pressure dependences have not been addressed. Lacking the needed data base, pressure and temperature scaling parameters measured under substantially higher temperature and pressure conditions than prevail in the normal atmosphere have been the only ones available for use in modeling the water vapor continuum absorption in the 3- to 5-micrometer window [2]. The validity of using these scaling parameters has been seriously questioned by the factor of 2 difference between predicted strengths and previous measurements performed by the ASL for 14.3 torr of water vapor air broadened to 760 torr at 23°C [1]. This questioning was the impetus for performing the extensive pressure dependence study of the water vapor continuum in the 3.5- to 4.0-micrometer spectral region at 25°C.

Laboratory measurements are contained herein which improve predictive modeling of the pressure dependence of the 3- to 5-micrometer water vapor continuum absorption at ambient temperatures (i.e., at naturally occurring temperatures between 0°C and 40°C). Long-path absorption cell measurements on deuterium depleted water vapor samples have resulted in the first measures of the self-broadening contribution as well as the foreign-to-self-broadening coefficient of the 3.5- to 4.0-micrometer water vapor continuum absorption at an ambient temperature. These data can be used to infer that the ambient temperature water vapor continuum absorption in this spectral region has contributions from two different sources. The first mechanism is due to far wing absorption and has substantial foreign gas broadening dependence. The second mechanism is less understood from the standpoint of the actual absorber but may be due to some form of aggregate-water-molecule with perhaps ionic bonding present. This second mechanism has little or no dependence upon foreign gas pressure and much stronger falloff with increasing temperature than the far wing contribution. These new measurements substantially increase the accuracy of the data base used in modeling of the effects of the atmosphere on Army and Department of Defense EO including HEL systems.

STATUS OF THE AMBIENT TEMPERATURE WATER VAPOR CONTINUUM

Throughout this report, transmittance is taken to be of the form $T = \exp(-k\ell)$, where k is an absorption coefficient expressed in km^{-1}

and ℓ is the pathlength in kilometers.

Since the water vapor continuum is a residual absorption in spectral regions between strongly absorbing bands (i.e., atmospheric windows), the absorption is relatively weak (a few percent/kilometers) yet important to the operation of many EO including HEL systems [3]. To understand what causes this absorption and hence accurately model it, extensive measurements of the pressure and temperature dependencies of the continuum must be made. The physical mechanism responsible for the water vapor continuum absorption in the infrared atmospheric windows still remains in question. Several recent measurements of the continuum in the 8- to 12-micrometer window imply, in part, the existence of an aggregate-water-molecule type of absorption (perhaps water dimers) [4,5] with strong temperature and weak foreign gas broadening dependencies. Measurements of Burch et al. [2] at elevated temperatures imply a far wing type continuum in the 3- to 5-micrometer window with weaker temperature and stronger foreign gas broadening dependencies. (However, the Burch measurements do not extrapolate well to ambient temperatures, as is evidenced by the factor of 2 difference between predictions and previous ASL measurements [1].)

A detailed discussion of the functional form of the far wing type water vapor continuum has already been given elsewhere and will not be reiterated here [1]. The absorption coefficient was given as:

$$k_c(\nu, T) = n_s \left[C_s(\nu, T)\, p_s + C_f(\nu, T)\, p_f \right], \qquad (1)$$

where n_s is the number of water vapor molecules per cm^3, C_s and C_f have units $cm^2(\text{atm molecule})^{-1}$ and are frequency (ν) and temperature (T) dependent empirical parameters which qualify, respectively, self- and foreign-broadening contributions. p_s and p_f are, respectively, self (i.e., water vapor) and foreign gas partial pressure in atmospheres. In the following discussions the pressure will be given in torr instead of atmospheres with a corresponding change in the units of C_s and C_f. An important quantity needed to accurately model this absorption as a function of pressure is the ratio of the foreign-to-self-broadening coefficients C_f/C_s. In the 8- to 12-micrometer window, the ratio of C_f/C_s is measured to be at most 0.005, with a lower bound of C_f/C_s approaching zero [6], which is atypical of far wing type absorption. The elevated temperature measurements of Burch give a value of C_f/C_s of 0.12 in the 3- to 5-micrometer window which is consistent with the far wing explanation of the water vapor continuum. Increased absorption in the wings of water lines (or "super"-Lorentz line shapes) has been measured for water vapor on either side of the 3- to 5-micrometer window [7,8], lending further support to the far wing explanation for a portion of the continuum absorption observed in water vapor.

ANALYTICAL AND EXPERIMENTAL APPROACH

As a first attempt to explain the factor of 2 discrepancy between the Burch predictions for the ambient temperature water vapor continuum absorption and the ASL measurements, the pressure dependence of the absorption needs to be investigated. This investigation entails measuring the self-broadening contribution C_s as well as the foreign-to-self-broadening ratio C_f/C_s at ambient temperatures. For the present measurements, midlatitude summer (MLS) type conditions were used: 14.3 torr of water vapor at 25°C with varying partial pressures of air (80/20 mixture of N_2/O_2). If the Burch elevated temperature value for C_f/C_s of 0.12 is correct, then the self-term $n_s C_s P_s$ (no foreign broadening) would contribute about one-seventh of the total (self- and foreign-broadened) absorption at standard pressure (760 torr), while the total absorption would be increased by 50 percent if the total pressure is air broadened to 1-2/3 atmospheres (about 1260 torr). Accordingly the measurement scheme was to measure the absorption of 14.3 torr of water vapor air broadened in 250-torr intervals from 0 to 1250 torr. From these measurements the self-contribution C_s as well as the foreign-to-self-broadening ratio C_f/C_s can be deduced.

The water vapor continuum absorption measurements were performed by using an experimental setup described elsewhere [1,9,10]. A line tunable 3.5- to 4.0-micrometer DF laser is used in conjunction with a 21-m long-path absorption cell with conventional White-type optics. A fully automated path differencing technique [11] was used to perform these measurements - the path difference being 1512 m. The cell was maintained at the summer time laboratory nominal temperature of 25°C.

These measurements are not easy to perform for several reasons. The absorption of air broadened water vapor at each laser line is due not only to the water vapor continuum but also to line absorptions from H_2O and HDO molecules and, near 4.0 micrometers, substantial absorption arises from the nitrogen continuum especially at the higher buffering pressures. The problem of relatively strong HDO line absorption is somewhat alleviated by using (as in previous experiments) [1,12] a deuterium depleted water sample with one-fiftieth the normal HDO concentration. Even with deuterium depleted water, predictions must be obtained for the line absorptions at each laser line for each buffering pressure and subtracted from the total absorption to obtain the continuum contribution. These calculations are performed by using the AFGL line parameter compilation [13], and details of the procedures are given elsewhere [1]. The problem of the nitrogen continuum absorption was essentially eliminated through the usual procedure of ratioing the transmission through an atmosphere with the deuterium depleted water vapor present to an atmosphere without the water vapor. One salient feature remained, however, in that the weak laser signals at the ends of a series, in particular the $v_3 \rightarrow v_2$ laser line series near 4.0

micrometers, were substantially attenuated by the nitrogen absorption resulting in more data scatter.

A second and even more complicating factor is the magnitude of the water vapor continuum between 3.5 and 4.0 micrometers. The relatively weak continuum absorption does not have spectral fine structure; hence, high resolution and spectral scanning are not required, but high-sensitivity absorption measurements are. The measurement of ambient temperature water vapor continuum cannot be simplified by significantly increasing the water vapor content (and hence the magnitude of the weak absorption) because condensation will result. This condensation must be strictly avoided to perform accurate long-path absorption cell measurements. Bearing in mind these factors, the measurements performed during this study were difficult to obtain even with the sophisticated long-path absorption cell used. Without the automated path differencing technique used [11], it may not have been possible to perform this study at all.

DISCUSSION OF EXPERIMENTAL RESULTS

The absorbing and nonabsorbing absolute cell transmittances represented by (as discussed in ref 14) T_a [N, 1] and T_n [N, 1], respectively, were measured at 25°C for a 37-spot (i.e., N = 37) multipath in a fully automated 21-m long-path absorption cell (i.e., L = 21 m) for 26 DF laser lines ranging in frequencies from $P_{1-0}(2)$ at 2862.646 cm^{-1} to $P_{3-2}(11)$ at 2471.243 cm^{-1}. For the absorbing case, a pressure of 14.3 torr of deuterium depleted water vapor was used and replaced by 14.3 torr of O_2 for the nonabsorbing case. Six absorbing and nonabsorbing cases were investigated with foreign gas (80/20 mixture of N_2/O_2) buffer pressures varying in 250-torr intervals from 0 to 1250 torr. The cell total pressures were thus 14.3, 264.3, 514.3, 764.3, 1014.3, and 1264.3 torr. The water vapor continuum absorption coefficients for each cell pressure are fundamentally obtained by applying the Lambert-Beer expression $T = \exp(-k\Delta\ell)$ to the absolute transmittance of the water vapor with a $\Delta\ell$ path difference using $T = T_a$ [37,1] / T_n [37,1] and then subtracting the water line absorption predictions [1] obtained by using the AFGL tape [13].

In these measurements the nonabsorbing absolute cell transmittance T_n [37,1] was not truly nonabsorbing because of the presence of the nitrogen continuum near 4.0 micrometers. Measurements of the nitrogen continuum have already been made by Burch [2] and can be used to obtain a correction factor (') to make the T_n [37,1] values truly nonabsorbing transmittances T_n [37,1]' for each cell pressure. The same factor of course must also be used on the absorbing T_a [37,1] values corresponding to each cell pressure so as not to alter the value of the absolute transmittance of the water vapor $T = T_a$ [37,1]'/T_n [37,1]'. Before

such a correction was performed, the nitrogen continuum absorption was checked by comparing the absolute cell transmittance for a 1512-m path difference with 1250 torr of N_2 to 1250 torr of an O_2-A_r mixture (a pure O_2 atmosphere was not used) against the Burch measurements. Three laser lines were used $P_{3-2}(11)$, $P_{3-2}(10)$, and $P_{3-2}(9)$. The results were about 10 percent below Burch but with overlapping error bounds. Hence Burch's values were used to correct the absolute cell transmittance values.

The reason for the above discussion of correcting for the nitrogen continuum absorption will now be made clear. The measured value of the water vapor transmittance T when obtained by using path differencing exhibits almost no long-term drift error commonly associated with long-path absorption cell measurements and hence is nearly time independent [14]. The values of T_a [37,1] and T_n [37,1] at each cell total pressure should also remain time independent barring a major experimental setup change. This proved to be the case during this experiment. Now, there is no a priori reason why the nitrogen continuum corrected T_n [37,1]' values should not change with total cell pressure. Increased cell pressure, though nonabsorbing, does spread the laser beam and has the net effect of reducing the cell output signal. Typically 5 to 10 percent signal losses were experienced by the laser line frequencies in a monotonic fashion as the nonabsorbing gas pressure was changed from 14.3 torr to 1264.3 torr. The loss experienced was not consistent from laser line to laser line (perhaps beam geometry related) but did vary essentially linearly for each line with total cell pressure. Hence, a least squares linear fit was used on all of the T_n[37,1]' values for the six different cell pressures to obtain more accurate values for T_n[37,1]' for each cell pressure. There was some indication that the Burch nitrogen continuum absorption values were slightly high since the T_n [37,1]' values for laser lines near 4.0 micrometers exhibited essentially no loss with increasing cell pressure indicating that the N_2-corrections overcorrected and eliminated these effects. Examples with and without the nitrogen continuum present, $P_{3-2}(9)$ and $P_{1-0}(4)$, respectively, are given in the upper plots of figures 1 and 2.

Before the absorbing absolute cell transmittance values T_a [37,1] could be analyzed, they had to be corrected for nitrogen continuum absorption plus H_2O and HDO line absorptions so as to reflect only a transmittance loss due to the water vapor continuum before ratioing them to the corresponding T_n [37,1]' values. These transmittance values are denoted as T_a[37,1]". However, using the same kind of linear smoothing on the absorbing absolute cell transmittance values T_a [37,1]" as was used on the T_n [37,1]' values is not strictly valid, since if equation (1) is correct, the absorption coefficient, not absolute cell transmittance, is linear with foreign broadening pressure. Fortunately,

since the absorption coefficients are small (a few percent/kilometer), the absolute transmittance values are very nearly equal to 1 minus the absorption coefficient so that a linear fit could be applied to the absorbing absolute cell transmittance values T_a [37,1]" as well, to increase the accuracy of the values at each cell pressure (see middle plots of figures 1 and 2).

Taking the ratio of the linear curve fit values of T_a [37,1]" to T_n [37,1]' for a given cell pressure yields the absolute transmittance due to the water vapor continuum absorption over the 1.512-km path difference. The corresponding per kilometer absorption coefficients can then be calculated for each of the six cell pressures used by dividing -ln[T] by the path difference of 1.512 km. A linear fit with respect to foreign broadening pressure was again applied to these values for each laser line to obtain more accurate values (see lower solid line plots of figures 1 and 2). The elaborate scheme of data reduction is designed to obtain the best possible values for the weak self-contribution to the water vapor continuum absorption and hence an accurate foreign-to-self-broadening coefficient. The absorption coefficients for all 26 laser lines are listed in table 1 and are plotted in figures 3 and 8 for each cell pressure used and are compared to the Burch extrapolations (solid curves). The self-contribution shown in figure 3 is weak (a few percent/kilometer) but not nearly as weak as the extrapolated values obtained from the elevated temperature data of Burch. In fact, the absorption is strong in comparison. Also, note that the factor of 2 difference observed previously at 23°C [1] was still present in the 25°C data at 764.3 torr total pressure. A comparison between the present work at 25°C and the previous measurement of the water vapor continuum absorption at 23°C is shown in figure 9. The present data are in general about 15 percent lower but well within the measurement uncertainty of about 0.01 km^{-1}. Finally, comparison of the 14.3 torr data and 1264.3 torr data indicates much weaker dependence of the water vapor continuum on foreign broadening pressure than Burch measured at 155°C.

Before the actual value of the foreign-to-self-broadening is obtained, further data reduction is necessary. At each foreign broadening pressure a quadratic least squares fit of the absorption coefficient versus frequency was performed by using the data at all 26 laser frequencies. These fits are represented by the dashed lines in figures 3 to 8 and all have very similar shapes, including minimums near the same frequency. The values at each laser frequency are listed in parentheses in table 1 and shown as a dashed line linear fit for laser lines $P_{1-0}(4)$ and $P_{3-2}(9)$, respectively, in the lower plots of figures 1 and 2. An iterative process could have been used to make the curves at each pressure have exactly the same shape by performing a linear least squares fit to the quadratic curve fit values at each laser frequency for the six foreign broadening pressures.

These values could then be used to obtain a new quadratic fit of absorption versus frequency for the six foreign broadening pressures, and the process repeated. This process was not pursued because the first iteration produced only minimal changes from the curve fits shown in figures 3 to 8. Note that the quadratic fits used on the data were not perfect shape representations of the continuum absorption. The ends of the curves appear to rise too rapidly especially at the higher broadening pressures. As a result, extrapolation outside the 3.5- to 4.0-micrometer region will yield only approximate values for the water vapor continuum absorption.

The foreign-to-self-broadening coefficient B* can now be calculated for each laser frequency, but first it should be better defined. Using $B^* = C_f/C_s$, equation (1) can be rewritten for a given laser line at 25°C and 14.3 torr of water vapor as

$$k_c(p_f) = n_s C_s (14.3 + B^* p_f). \qquad (2)$$

Since the curve fit values of $k_c(p_f)$ vary linearly with foreign broadening pressure (see bottom dashed line plots in figures 1 and 2), only values of $k_c(0)$ and $k_c(1250)$ need be used to obtain the values of B*. The resulting expression for B* is

$$B^* = \frac{k_c(1250) - k_c(0)}{k_c(0)} \left(\frac{14.3}{1250}\right) = 0.01144 \frac{k_c(1250) - k_c(0)}{k_c(0)} \qquad (3)$$

Values for the foreign-to-self-broadening coefficients are given in table 2 and figure 10 for all 26 laser lines. Column 2 represents B* values obtained by using the absorption coefficients after the quadratic curve fit was applied to the sets of data at $p_f = 0$ and 1250 torr. There is something peculiar about these B* values of foreign-to-self-broadening which cannot be explained even when the 0.01 km^{-1} measurement uncertainty of the absorption coefficients is taken into account. From figure 10, B* appears to be frequency dependent, showing smaller values near 2800 cm^{-1} than at 2600 cm^{-1}. Column 3 represents values of B* before curve fitting, the average value for the first being 0.018 and the second 0.010. There is a problem with taking a simple average because the values of B* at laser lines where $k_c(0)$ is small have large uncertainties due to the $1/k_c(0)$ dependence of B*. Hence a weighted average would be more appropriate, or

$$\bar{B}^* = \frac{\sum_{i=1}^{26} B_i^* \; k_c(0)_i}{\sum_{i=1}^{26} k_c(0)_i} \qquad (4)$$

where the index represents the i^{th} laser line. The $\bar{B}^*$ values for both sets of B^* values in columns 2 and 3 of table 2 gave the same weighted average value of 0.011 which is an order of magnitude smaller than the elevated temperature Burch value of 0.12.

One can conclude that the 3.5- to 4.0-micrometer water vapor continuum exhibits similar behavior to the 8- to 12-micrometer region where the continuum is thought to be due to aggregate-water-molecule absorption. One should not jump to the conclusion that there is no far wing type absorption however. Note that 65°C foreign gas broadened water vapor continuum absorption data measured at ASL supports the 0.12 value of foreign-to-self-broadening ratio rather than the 0.011 measured here at 25°C.

AMBIENT TEMPERATURE CONTINUUM MODELING

One could stop the discussion at this point and allow the readers to model for themselves the measured values of self-contribution to the water vapor continuum and the foreign-to-self-broadening ratio at ambient temperature. A method will, however, be conjectured herein which should be taken as preliminary since, though it is consistent with the results obtained thus far, it requires verification by the extensive temperature dependent study of the water vapor continuum absorption between 25°C and 65°C now being pursued at the ASL. The reason for presenting the method of course is that the authors feel that it will yield more accurate predictions than any of the presently existing models.

First the authors feel that the water vapor continuum has at least three significant terms instead of the two shown in equation (1). There should be an additional term representing a possible aggregate-water-molecule absorption (perhaps with ionic bonding) [15] of the form $n_s C_s^A p_s$ which results in a new expression for k_c (ν, T) of

$$k_c\ (\nu,\ T) = n_s \left[C_s^W\ (\nu,\ T)\ p_s + C_f^W\ (\nu,\ T)\ p_f + C_s^A\ (\nu,\ T)\ p_s\right] \qquad (5)$$

where the superscripts W and A represent, respectively, far wing and aggregate contribution to the continuum absorption. The temperature dependence (as discussed later) will not be the same for the different terms. The justification for the expression is obtained by observing the behavior of the term C_s^A (ν, T). If the aggregate absorption in the 3.5- to 4.0-micrometer region is similar to that in the 8- to 12-micrometer window, there will be little if any change in the absorption with foreign broadening pressure [6]. The $n_s C_s^A$ (ν, T) p_s term gives this behavior as well as a squared dependence on the self-pressure since $n_s \sim p_s$.

Values of $n_s C_s^A (\nu, T)\ p_s$ can be obtained for each laser line and foreign broadening pressure used by assuming that the Burch extrapolation is valid and represents only far wing type absorption which can be subtracted from the measured continuum absorption coefficients. A set of the Burch predictions for the far wing continuum contribution $n_s C_s^W (p_s + 0.12\ p_f)$ for 14.3 torr water vapor at 25°C buffered by the various foreign broadening pressures used is given in table 3 for all 26 laser lines. The residual absorption taken as the value of $n_s C_s^A p_s$ was obtained by subtracting the Burch values in table 3 from the corresponding curve fit values of total water vapor continuum absorption given in parentheses in table 1. The resulting set of $n_s C_s^A p_s$ values is given in table 4. At each laser line the aggregate-water-molecule absorption contribution $n_s C_s^A p_s$ is nearly independent of foreign broadening pressure within the experimental uncertainty of the measured absorption coefficients and the Burch predictions. This pressure independence is only borderline near 3.5 micrometers. However, this is the region where the ASL 65°C data did not conclusively support the Burch extrapolations. Even so it is still reasonable until a better data base is available to use the average of the six residual absorption values at each laser frequency listed in column 7 of table 4 as the value of $n_s C_s^A p_s$ at 25°C.

At this point the temperature dependence of the water vapor continuum will be discussed briefly. The two far wing type terms (superscript W) in equation (5) are modeled by using the Burch temperature dependence which has the form

$$\frac{T_o}{T}\ \exp\left[-m\left(\frac{1}{T_0}\ -\frac{1}{T}\right)\right]$$

where the T_0/T part is from the n_s term, the exponential is due to C_s^W and C_f^W, and the coefficient m is found to be frequency dependent [16]. The C_s^A temperature dependence in the third term of equation (5) is not known at this time but should cause the aggregate absorption to become small at 65°C. The absorption should be far wing type dominated at 65°C since the absorption is dominated by the foreign pressure broadened term $n_s C_f^W p_f$ in equation (5) as evidenced by the agreement of the Burch predictions and the ASL foreign broadened measurements at 65°C. The question of how much aggregate absorption is present at 65°C is still not clear at this point.

Comparison of the previous ASL 23°C water continuum measurement with the present one is beneficial. In table 5 the Burch water vapor continuum measurement extrapolations for 14.3 torr water vapor buffered to 760 torr total pressure at 23°C (column 3) are subtracted from the ASL measurement curve fit values (column 2) to obtain the aggregate-water-molecule absorption at 23°C (column 4). The 23°C values are

within the measurement error of the 25°C aggregate-water-molecule absorption values (column 5) obtained in this study; consequently, no meaningful temperature dependence can be derived from these sets of measurements. It is at least pleasing that the 25°C values are in general smaller than the 23°C, thus hinting at a falloff of the absorption with increasing temperature as expected. What can be done is to average the two sets of values to arrive at values of $n_s C_s^A p_s$ to be used for temperatures around 24°C as in column 6 of table 5. The total continuum absorption (column 8) is obtained by adding the Burch predictions (column 7) to column 6.

In review, the proposed model for the ambient temperature has several new features. First, the water vapor continuum absorption in the 3- to 5-micrometer window is assumed not to be solely due to self- and foreign-broadened far wing absorption but has an additional contribution due to a proposed aggregate-water-molecule type absorption expressed as $n_s C_s^A p_s$ with essentially no foreign broadening dependence. Second, values for this aggregate contribution can be obtained by assuming the Burch extrapolation of the far wing contribution to the water continuum based on higher temperature and pressure measurements to be valid at ambient temperatures. The Burch extrapolated values can then be subtracted from the total measured continuum absorption to give values for $n_s C_s^A p_s$. Third, the aggregate contribution must decrease more rapidly than the far wing contribution between 25°C and 65°C since the water vapor continuum is far wing dominated at 65°C. The exact expression for this dependence cannot be adequately defined until further measurements are performed. Last, bearing in mind the above, representative values of $n_s C_s^A p_s$ are obtained by averaging available 23°C and 25°C data to obtain estimates for the aggregate contribution around 24°C. Values for the water vapor continuum absorption can be obtained for temperatures around 24°C by adding the Burch far wing absorption for this temperature to the 24°C value of $n_s C_s^A p_s$.

The most significant departure of this new modeling scheme for the water vapor continuum at ambient temperatures will now be discussed. The water vapor continuum will not vary as expected with changes in the partial pressure of water at 760 torr total pressure atmospheres. The 24°C values of $n_s C_s^A p_s$ column 6 of table 5 and the Burch predictions are used to model equation (5) for relative humidities ranging from 10 to 100 percent in table 6 for 760 torr total pressure at 24°C. The predicted absorption values are more strongly dependent on water vapor partial pressure than previously thought because of the reduced dependence of the water vapor continuum absorption on foreign pressure broadening. Also, the absorption will not fall off as rapidly with decreasing buffer pressure as was expected with increasing altitude. Unfortunately, modeling of the water vapor continuum absorption as a function of altitude is not practical at this time because of the wide fluctuation of temperature with changes in altitude.

REFERENCES

1. White, K. O., W. R. Watkins, C. W. Bruce, R. E. Meredith, and F. G. Smith, 1978, "Water Vapor Continuum Absorption in the 3.5μm to 4.0μm Region," ASL-TR-0004, Atmospheric Sciences Laboratory, White Sands Missile Range, NM.

2. Burch, D. E., D. A. Gryvnak, and J. D. Pembrook, 1971, "Investigation of the Absorption of Infrared Radiation by Atmospheric Gases: Water, Nitrogen, Nitrous Oxide," AFCRL-71-0124, Hanscom AFB, MA.

3. Watkins, W. R., K. O. White, C. W. Bruce, D. L. Walters, and J. D. Lindberg, 1977, "Measurements Required for Prediction of High Energy Laser Transmission," ECOM-5834, Atmospheric Sciences Laboratory, White Sands Missile Range, NM.

4. Montgomery, G. P. Jr., 1977, "Temperature Dependence of Infrared Absorption by the Water Vapor Continuum Near 1200 cm^{-1}," GMR-2562, General Motors, Research Laboratories, Warren, MI.

5. Coffey, M. J., 1977, "Water Vapor Absorption in the 10-12 μm Atmospheric Window," Quart. J. Roy. Meteorol. Soc., 103:685.

6. Roberts, R. E., J. E. A. Selby, and L. M. Biberman, 1976, "Infrared Continuum Absorption by Atmospheric Water Vapor in the 8-12 μm Window," Appl. Opt. 15:2085.

7. Long, R. K., F. S. Mills, and G. L. Trusty, 1973, "Experimental Absorption Coefficients for Eleven CO Laser Lines," The Ohio State University Electroscience Laboratory Report No. 3271-5.

8. Watkins, W. R., R. L. Spellicy, K. O. White, B. Z. Sojka, and L. R. Bower, 1978, "Water Vapor Absorption Coefficients at HF Laser Wavelengths. Part I: Atmospheric Conditions Corresponding to Altitudes up to 7 km," ASL-TR-0007, Atmospheric Sciences Laboratory, White Sands Missile Range, NM.

9. Watkins, W. R., 1976, "Improvements in Long Path Absorption Cell Measurements," ECOM-5586, Atmospheric Sciences Laboratory, White Sands Missile Range, NM.

10. White, K. O., and W. R. Watkins, 1975, "Absorption of DF Laser Radiation by Propane and Butane," ECOM-5563, Atmospheric Sciences Laboratory, White Sands Missile Range, NM.

11. Watkins, W. R., and R. G. Dixon, 1977, "Automation of Long Path Absorption Cell Measurements," ECOM-5821, Atmospheric Sciences Laboratory, White Sands Missile Range, NM.

12. Watkins, W. R., and K. O. White, 1977, "Water-vapor-continuum Absorption Measurements (3.5 - 4.0 μm) Using HDO-depleted Water," Opt. Let., 1:31.

13. McClatchey, R. A., W. S. Benedict, S. A. Clough, D. E. Burch, R. E. Calfee, K. Fox, L. S. Rothman, and J. S. Garing, 1973, "AFGL Atmospheric Absorption Line Parameter Compilation," AFCRL-TR-73-0096.

14. Watkins, W. R., 1976, "Path Differencing: on Improvement to Multi-pass Absorption Cell Measurements," Appl. Opt. 15:16.

15. Carlon, H. R., "A Molecular-Cluster (Ion Hydrate) Explanation of the Infrared Water Vapor Continuum Absorption," (to be submitted for Publication) Research Division, Chemical Systems Laboratory, Aberdeen Proving Ground, MD, 21010.

16. Meredith, R. E., Private Communication, Letter Report No. 1-161-00-700-00(3), 10 January 1977, Science Applications, Inc., 15 Research Dr., P. O. Box 328, Ann Arbor, MI, 48107.

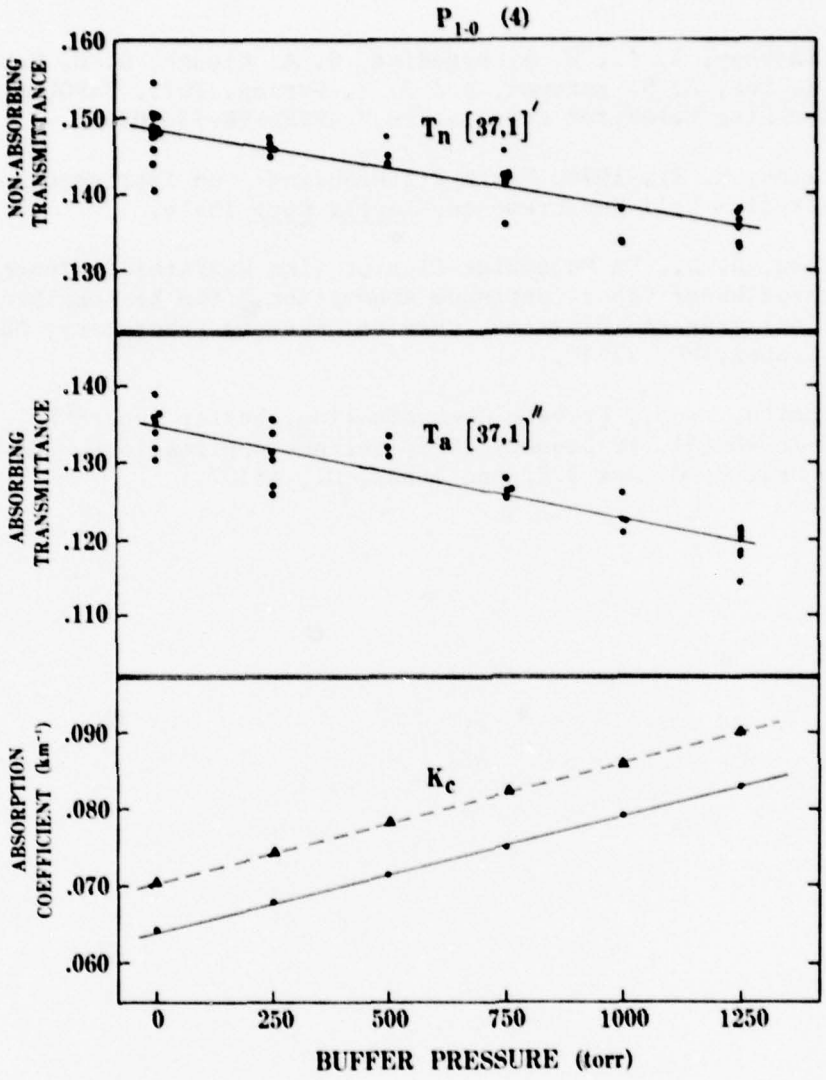

Figure 1. Cell transmittances (for a 1.512 km path difference) and corresponding water vapor continuum absorption coefficients at 25°C for DF laser line $P_{1-0}(4)$ at 2816.380 cm^{-1}. Upper plot: Absolute non-absorbing cell transmittance data taken for 14.3 torr of O_2 buffered by 0,250,500,750,1000, and 1250 torr of air (80/20 mixture of N_2/O_2). Side-by-side data represent multiple values at same buffer pressure. No N_2 continuum correction needed. Solid line represents linear least squares fit to data. Middle plot: Absolute absorbing cell transmittance data taken under same buffering conditions as above except 14.3 torr of deuterium depleted water vapor replaces the 14.3 torr of O_2. Data are corrected for H_2O and HDO line absorptions. Solid line represents linear least squares fit to data. Lower plots: Per km absorption coefficients for water vapor continuum obtained from transmittance data for each of the six buffering pressures. Circles represent absorption coefficients derived from the linear fits shown in the upper and middle plots. Solid curve is a linear least squares fit to the values thus obtained. Triangles represent absorption coefficients obtained from a least squares quadratic fit in frequency for 26 DF laser lines using the linear fit absorption coefficient (as above) at each of the six buffer pressures. Dashed line is a linear least squares fit to these values.

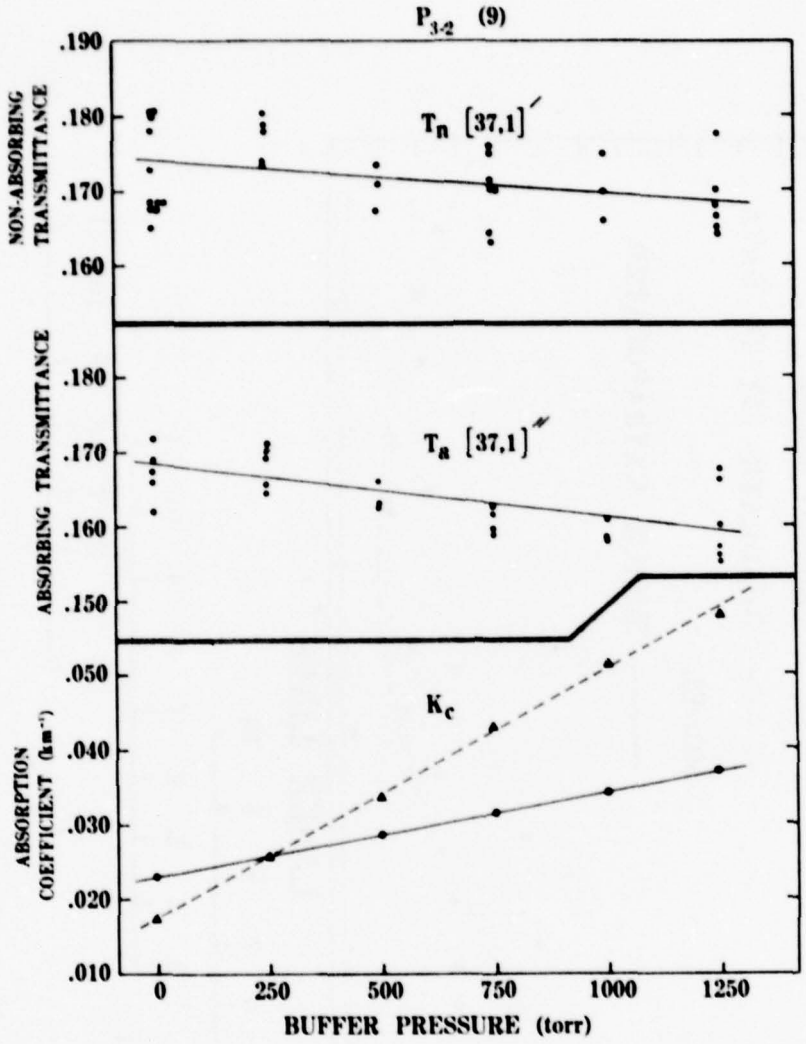

Figure 2. Cell transmittance (for a 1.512-km path difference) and corresponding water vapor continuum absorption coefficients at 25°C for DF laser line $P_{3-2}(9)$ at 2521.769 cm^{-1}. Upper plot: Absolute non-absorbing cell transmittance data taken for 14.3 torr of O_2 buffered by 0,250,500,750,1000, and 1250 torr of air (80/20 mixture of N_2/O_2). Side-by-side data represent multiple values at same buffer pressure. Data are corrected for N_2 continuum absorption. Solid line represents linear least squares fit to data. Middle plot: Absolute absorbing cell transmittance data taken under same buffering conditions as above except 14.3 torr of deuterium depleted water vapor replaces the 14.3 torr of O_2. Data are corrected for N_2 continuum and H_2O and HDO line absorptions. Solid line represents linear least squares fit to data. Lower plots: Per km absorption coefficients for water vapor continuum obtained from transmittance data for each of the six buffering pressures. Circles represent absorption coefficients derived from the linear fits shown in the upper and middle plots. Solid curve is a linear least squares fit to the values thus obtained. Triangles represent absorption coefficients obtained from a least squares quadratic fit in frequency for 26 DF laser lines using the linear fit absorption coefficient (as above) at each of the six buffer pressures. Dashed line is a linear least squares fit to these values.

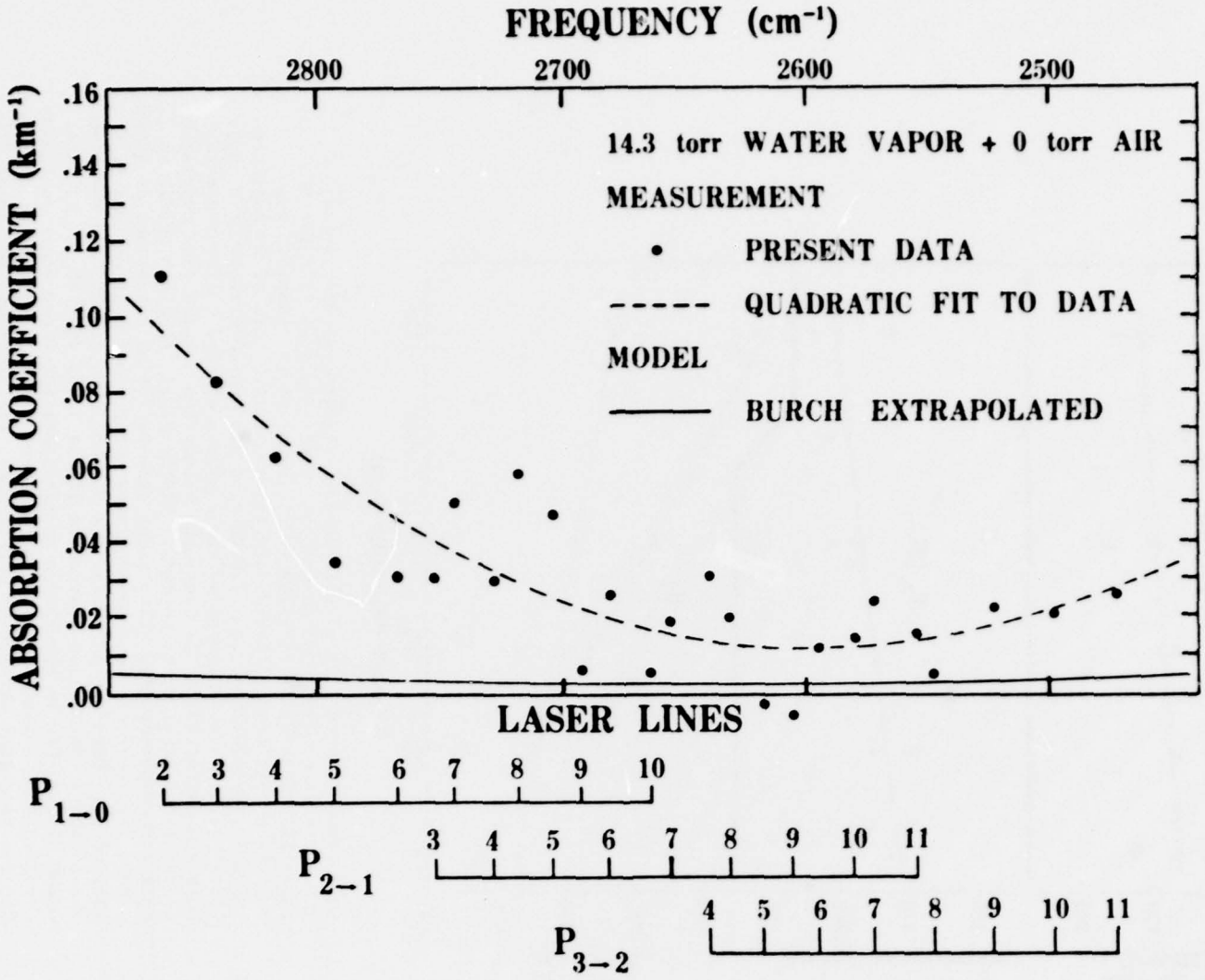

Figure 3. Comparison of measured water vapor continuum at 25°C to Burch extrapolation for 14.3 torr water vapor with no air broadening.

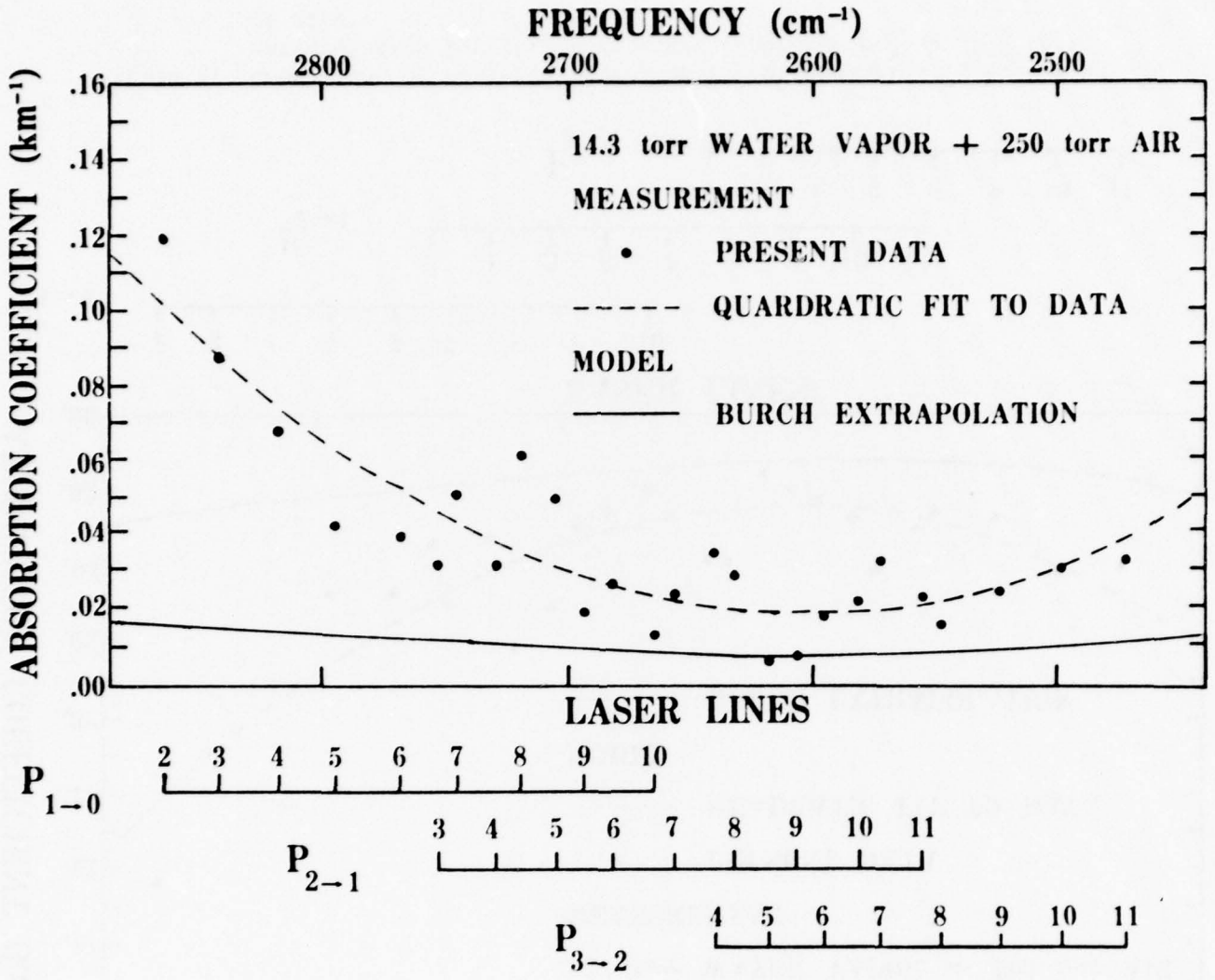

Figure 4. Comparison of measured water vapor continuum at 25°C to Burch extrapolation for 14.3 torr water vapor buffered by 250 torr of air.

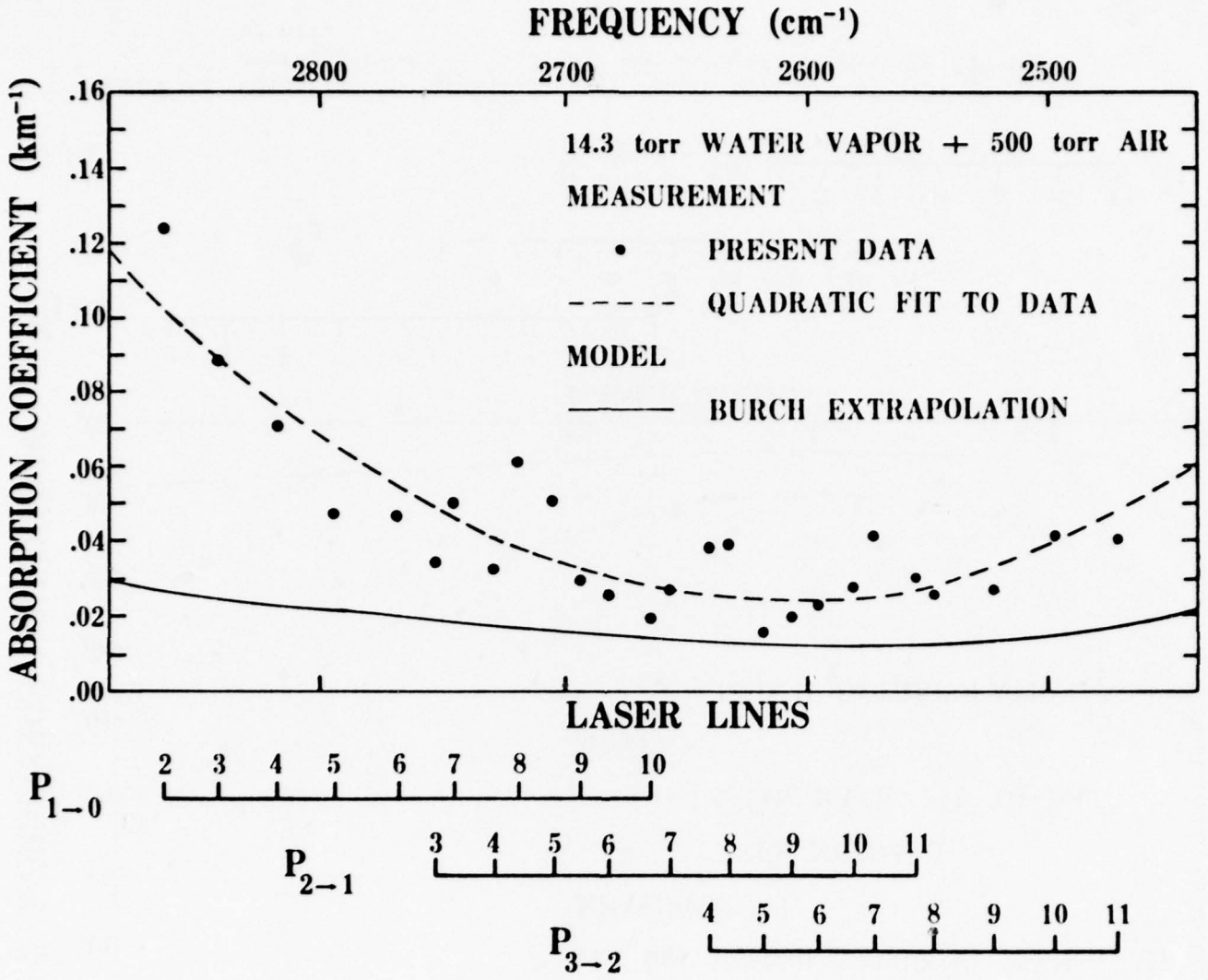

Figure 5. Comparison of measured water vapor continuum at 25°C to Burch extrapolation for 14.3 torr water vapor buffered by 500 torr of air.

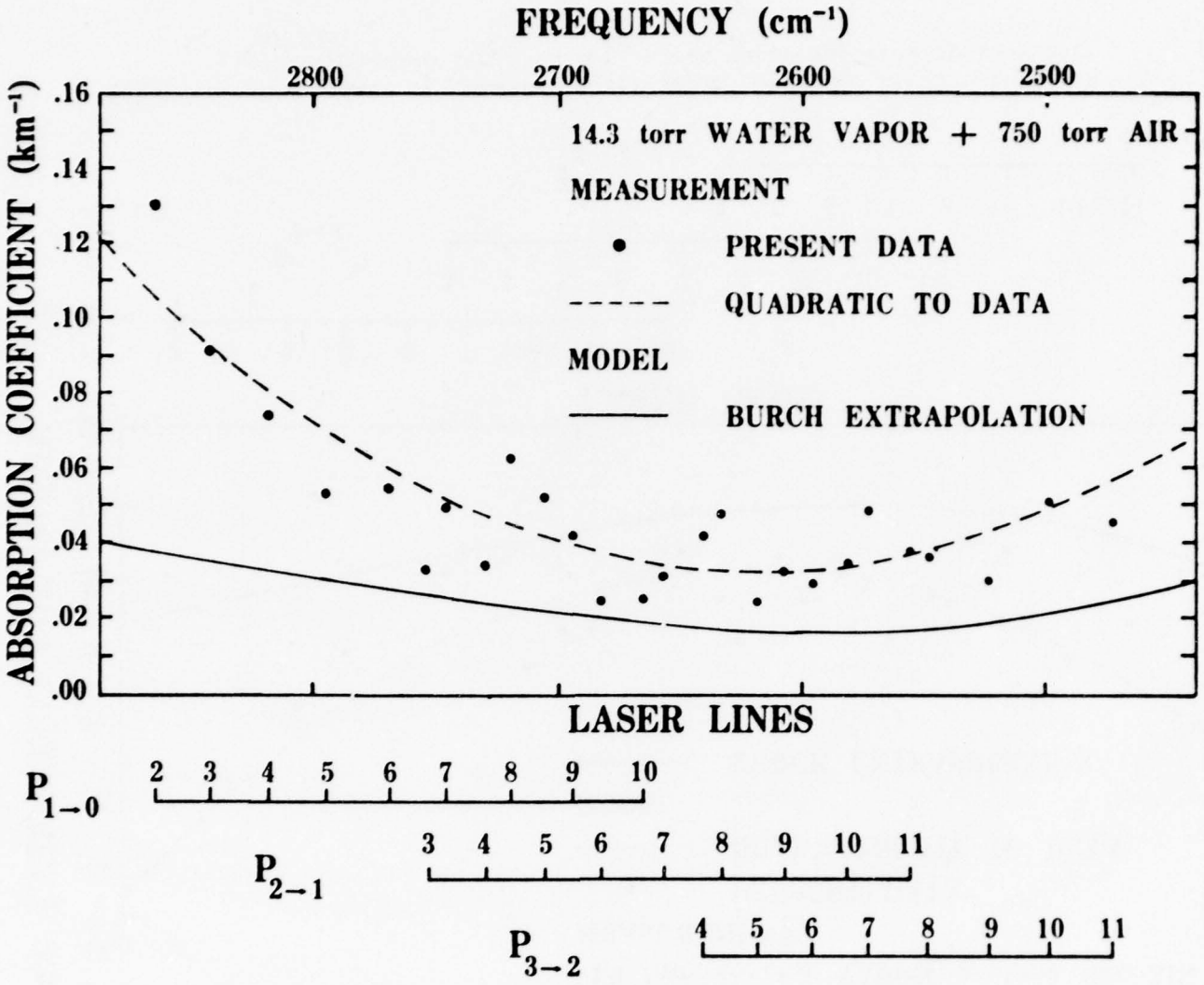

Figure 6. Comparison of measured water vapor continuum at 25°C to Burch extrapolation for 14.3 torr water vapor buffered by 750 torr of air.

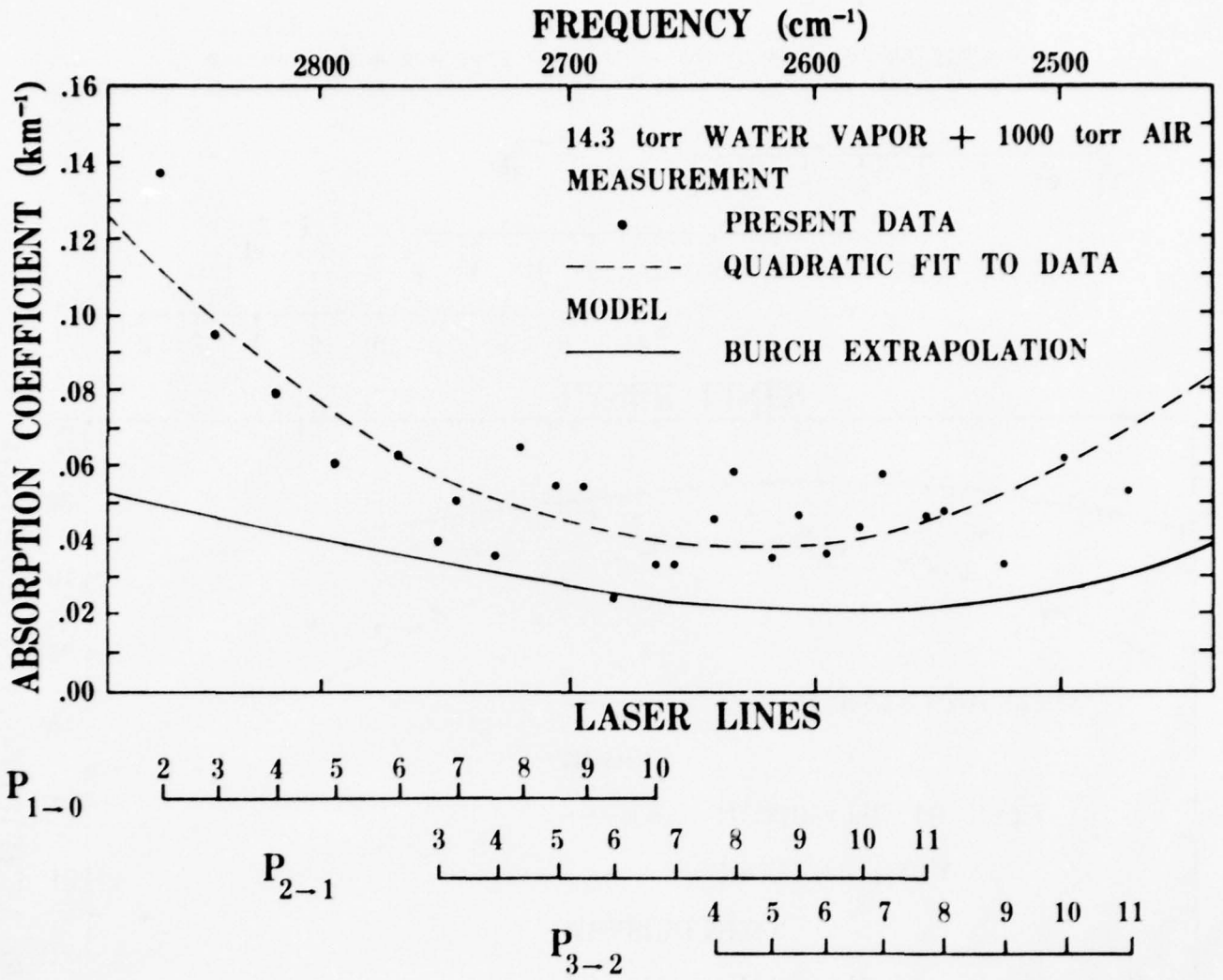

Figure 7. Comparison of measured water vapor continuum at 25°C to Burch extrapolation for 14.3 torr water vapor buffered by 1000 torr of air.

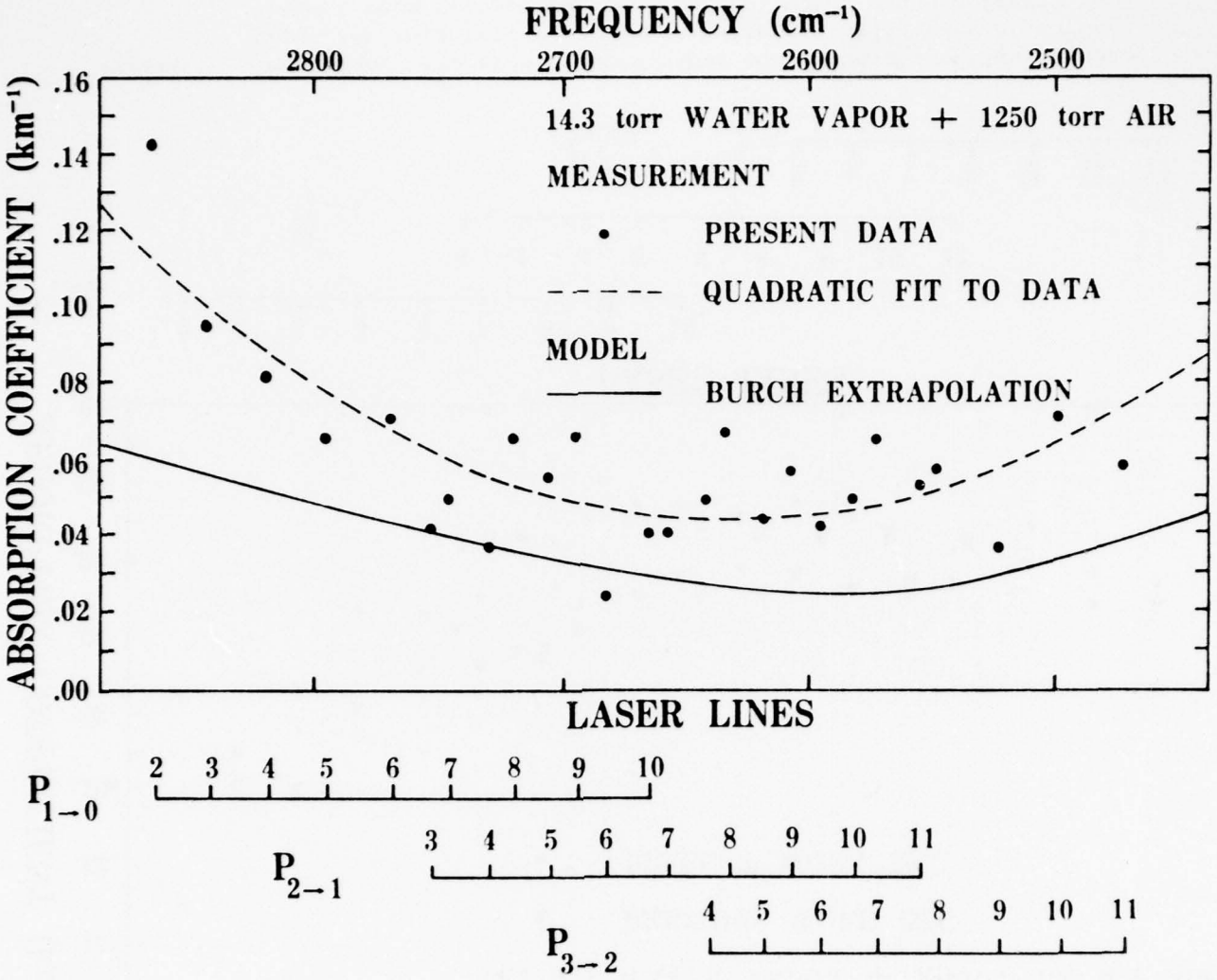

Figure 8. Comparison of measured water vapor continuum at 25°C to Burch extrapolation for 14.3 torr water vapor buffered by 1250 torr of air.

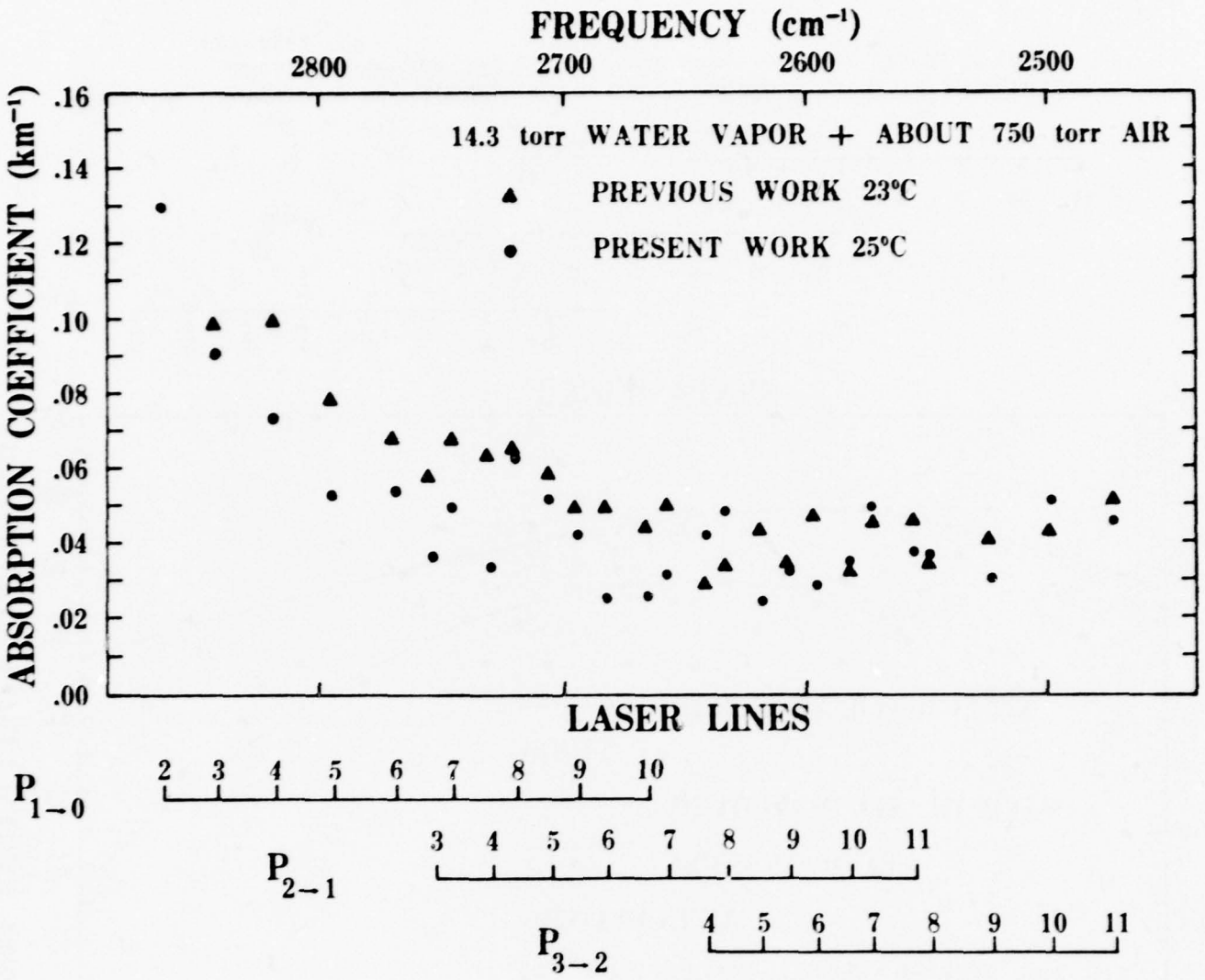

Figure 9. Comparison of previous water vapor continuum absorption measurements for 14.3 torr water vapor buffered to 760 torr at 23°C to present measurements for 14.3 torr of water vapor buffered to 764.3 torr at 25°C.

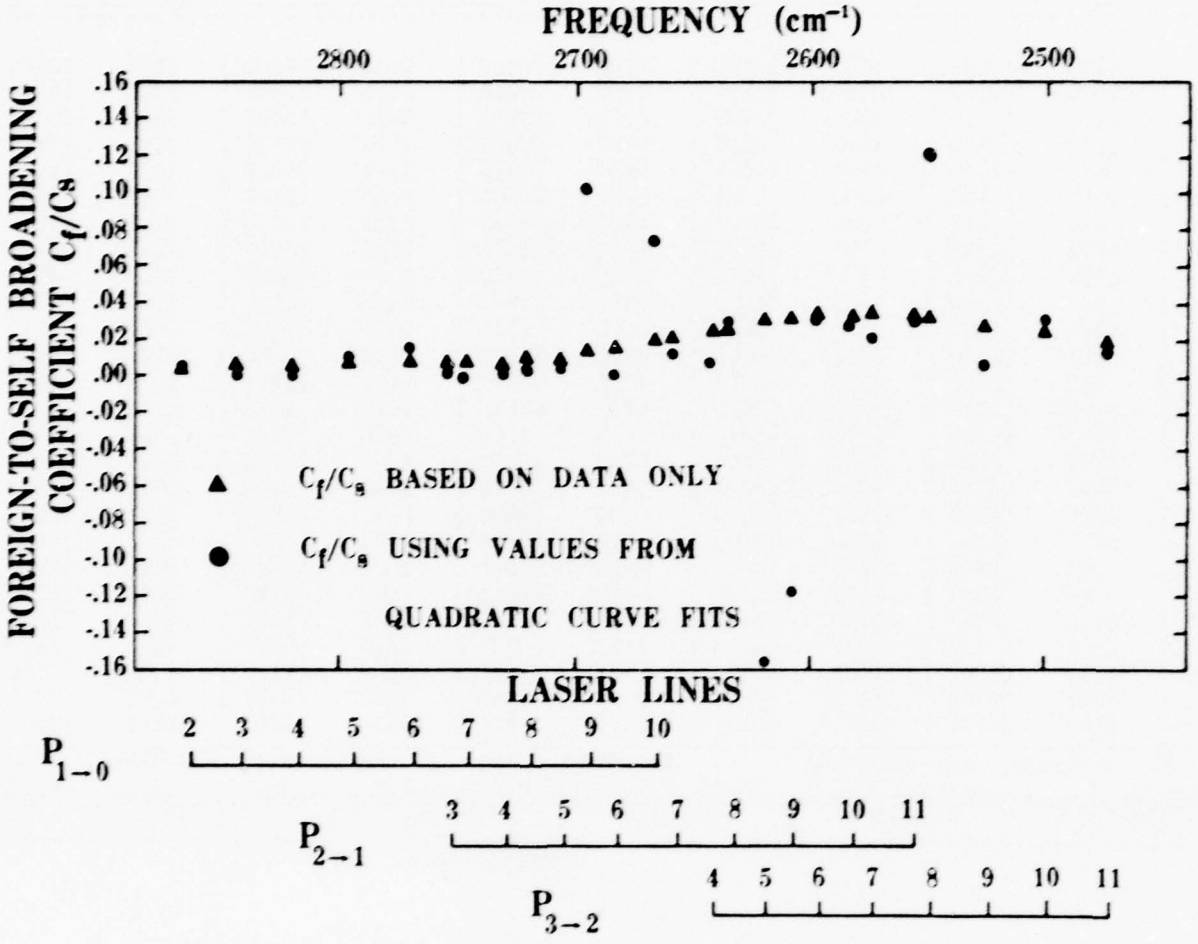

Figure 10. Comparison of the foreign-to-self-broadening coefficients (C_f/C_s) for the water vapor continuum at 26 DF laser lines before (circles) and after (triangles) curve fitting the measured absorption coefficients.

TABLE 1.
WATER VAPOR ABSORPTION COEFFICIENTS (km^{-1}) FOR 14.3 TORR WATER VAPOR
AT 25°C FOR SIX AIR BUFFER PRESSURES

Laser Line	Wavenumber (cm^{-1})	AIR BUFFER PRESSURE 0 Torr		250 Torr		500 Torr		750 Torr		1000 Torr		1250 Torr	
		Measured	Curve Fit	Measured	Curve Fit	Measured	Curve Fit	Measured	Curve Fit	Measured	Curve Fit	Measured	Curve Fit
$P_1(2)$	2862.646	.1123	(.0970)	.1190	(.1006)	.1257	(.1041)	.1324	(.1072)	.1391	(.1119)	.1458	(.1148)
$P_1(3)$	2839.791	.0850	(.0832)	.0873	(.0869)	.0895	(.0906)	.0917	(.0942)	.0940	(.0983)	.0962	(.1017)
$P_1(4)$	2816.380	.0640	(.0705)	.0678	(.0774)	.0716	(.0783)	.0754	(.0824)	.0792	(.0861)	.0839	(.0900)
$P_1(5)$	2792.434	.0353	(.0587)	.0415	(.0628)	.0478	(.0669)	.0541	(.0715)	.0604	(.0749)	.0667	(.0791)
$P_1(6)$	2767.968	.0310	(.0477)	.0392	(.0521)	.0473	(.0564)	.0554	(.0616)	.0635	(.0648)	.0717	(.0694)
$P_2(3)$	2750.093	.0307	(.0408)	.0329	(.0453)	.0351	(.0498)	.0373	(.0553)	.0395	(.0585)	.0417	(.0634)
$P_1(7)$	2742.997	.0507	(.0383)	.0506	(.0429)	.0506	(.0475)	.0505	(.0531)	.0505	(.0563)	.0504	(.0613)
$P_2(4)$	2727.308	.0305	(.0333)	.0319	(.0380)	.0333	(.0428)	.0348	(.0488)	.0362	(.0519)	.0376	(.0571)
$P_1(8)$	2717.538	.0596	(.0302)	.0610	(.0351)	.0624	(.0400)	.0639	(.0461)	.0653	(.0494)	.0667	(.0547)
$P_2(5)$	2703.998	.0479	(.0263)	.0496	(.0314)	.0513	(.0365)	.0529	(.0429)	.0546	(.0462)	.0562	(.0517)
$P_1(9)$	2691.608	.0065	(.0234)	.0186	(.0286)	.0307	(.0339)	.0428	(.0405)	.0549	(.0439)	.0670	(.0495)
$P_2(6)$	2680.178	.0272	(.0208)	.0267	(.0262)	.0263	(.0316)	.0258	(.0384)	.0253	(.0420)	.0248	(.0477)
$P_1(10)$	2665.218	.0054	(.0178)	.0125	(.0236)	.0195	(.0292)	.0265	(.0363)	.0336	(.0402)	.0406	(.0460)
$P_2(7)$	2655.863	.0192	(.0165)	.0236	(.0223)	.0279	(.0280)	.0322	(.0352)	.0336	(.0393)	.0409	(.0452)
$P_3(4)$	2640.075	.0311	(.0144)	.0348	(.0204)	.0385	(.0264)	.0422	(.0339)	.0459	(.0383)	.0496	(.0443)
$P_2(8)$	2631.066	.0200	(.0135)	.0297	(.0196)	.0393	(.0258)	.0490	(.0334)	.0586	(.0381)	.0683	(.0441)
$P_3(5)$	2617.386	-.0034	(.0125)	.0062	(.0189)	.0158	(.0252)	.0253	(.0331)	.0349	(.0381)	.0444	(.0442)
$P_2(9)$	2605.806	-.0062	(.0120)	.0069	(.0185)	.0200	(.0250)	.0331	(.0331)	.0462	(.0385)	.0593	(.0446)
$P_3(6)$	2594.197	.0113	(.0117)	.0176	(.0185)	.0240	(.0252)	.0303	(.0335)	.0366	(.0392)	.0429	(.0454)
$P_2(10)$	2580.095	.0144	(.0119)	.0216	(.0189)	.0287	(.0259)	.0359	(.0343)	.0430	(.0406)	.0502	(.0468)
$P_3(7)$	2570.522	.0250	(.0122)	.0332	(.0194)	.0414	(.0265)	.0497	(.0351)	.0579	(.0417)	.0661	(.0480)
$P_2(11)$	2553.951	.0155	(.0134)	.0231	(.0208)	.0308	(.0283)	.0384	(.0371)	.0460	(.0445)	.0536	(.0507)
$P_3(8)$	2546.373	.0048	(.0140)	.0154	(.0216)	.0261	(.0293)	.0368	(.0382)	.0474	(.0458)	.0581	(.0521)
$P_3(9)$	2521.769	.0228	(.0173)	.0256	(.0254)	.0285	(.0336)	.0313	(.0428)	.0342	(.0516)	.0370	(.0579)
$P_3(10)$	2496.720	.0206	(.0221)	.0309	(.0307)	.0412	(.0394)	.0515	(.0489)	.0618	(.0591)	.0721	(.0653)
$P_3(11)$	2471.243	.0271	(.0286)	.0335	(.0378)	.0399	(.0470)	.0463	(.0569)	.0527	(.0686)	.0591	(.0747)

TABLE 2.

FOREIGN-TO-SELF BROADENING COEFFICIENTS (C_f/C_s) FOR 14.3 TORR WATER VAPOR CONTINUUM AT 25°C

Laser Line	Foreign-to-self Broadening Coefficients from	
	Curve Fit	Measurements
$P_1(2)$	.0021	.0034
$P_1(3)$	.0025	.0015
$P_1(4)$	.0032	.0034
$P_1(5)$	.0040	.0102
$P_1(6)$	.0052	.0150
$P_2(3)$	.0063	.0041
$P_1(7)$	.0069	-.0001
$P_2(4)$	.0082	.0026
$P_1(8)$	.0093	.0014
$P_2(5)$	.0110	.0020
$P_1(9)$	.0128	.1065
$P_2(6)$	.0149	-.0010
$P_1(10)$	.0181	.0746
$P_2(7)$	.0199	.0129
$P_3(4)$	.0238	.0068
$P_2(8)$	.0259	.0276
$P_3(5)$	.0290	-.1608
$P_2(9)$	.0311	-.1209
$P_3(6)$	.0330	.0320
$P_2(10)$	.0336	.0284
$P_3(7)$	.0336	.0188
$P_2(11)$	.0318	.0281
$P_3(8)$	.0311	.1270
$P_3(9)$	.0268	.0071
$P_3(10)$	.0224	.0286
$P_3(11)$	.0184	.0135

TABLE 3.

BURCH EXTRAPOLATIONS FOR THE WATER VAPOR CONTINUUM ABSORPTION FOR 14.3 TORR WATER VAPOR AT 25°C FOR VARIOUS AIR BROADENING PRESSURES

Laser Line	Burch Extrapolated Absorption Coefficients (km^{-1}) For Different Air Broadening Pressures					
	0 Torr	250 Torr	500 Torr	750 Torr	1000 Torr	1250 Torr
$P_1(2)$	.0052	.0161	.0271	.0380	.0489	.0599
$P_1(3)$	.0049	.0152	.0255	.0358	.0461	.0564
$P_1(4)$	.0046	.0142	.0239	.0335	.0431	.0528
$P_1(5)$	.0043	.0132	.0222	.0311	.0401	.0491
$P_1(6)$	.0039	.0122	.0205	.0287	.0370	.0453
$P_2(3)$	.0037	.0115	.0192	.0270	.0348	.0425
$P_1(7)$	.0036	.0112	.0187	.0263	.0339	.0414
$P_2(4)$	.0034	.0105	.0176	.0248	.0319	.0390
$P_1(8)$	.0033	.0101	.0170	.0238	.0306	.0375
$P_2(5)$	.0031	.0095	.0160	.0225	.0289	.0354
$P_1(9)$	.0029	.0091	.0153	.0214	.0276	.0337
$P_2(6)$	.0028	.0087	.0147	.0206	.0265	.0324
$P_1(10)$	.0027	.0083	.0139	.0195	.0251	.0308
$P_2(7)$	.0025	.0080	.0135	.0189	.0244	.0298
$P_3(4)$	.0025	.0076	.0128	.0180	.0231	.0283
$P_2(8)$	.0024	.0074	.0124	.0175	.0225	.0275
$P_3(5)$	.0023	.0071	.0119	.0167	.0216	.0264
$P_2(9)$	.0022	.0069	.0115	.0162	.0209	.0255
$P_3(6)$	.0022	.0068	.0114	.0160	.0205	.0251
$P_2(10)$	.0022	.0068	.0115	.0161	.0208	.0254
$P_3(7)$	.0022	.0069	.0117	.0164	.0211	.0258
$P_3(11)$	.0023	.0072	.0121	.0170	.0219	.0268
$P_3(8)$	.0024	.0074	.0124	.0175	.0225	.0275
$P_3(9)$	.0026	.0082	.0137	.0193	.0248	.0304
$P_3(10)$	.0030	.0092	.0155	.0218	.0280	.0343
$P_3(11)$	.0033	.0104	.0174	.0244	.0314	.0385

TABLE 4.

AGGREGATE-WATER-MOLECULE CONTRIBUTION ($n_s C_s^A p_s$) TO THE WATER VAPOR CONTINUUM ABSORPTION (km^{-1}) FOR 14.3 TORR WATER VAPOR AT 25°C FOR VARIOUS AIR BROADENING PRESSURES

Laser Line	Aggregate-Water-Molecule Contribution Air Broadened by						Average Value of $n_s C_s^A p_s$ and Standard Deviation	
	0 Torr	250 Torr	500 Torr	750 Torr	1000 Torr	1250 Torr		
$P_1(2)$	.0918	.0845	.0788	.0692	.0630	.0549	.0737	±.0138
$P_1(3)$	.0783	.0717	.0651	.0584	.0522	.0453	.0618	±.0123
$P_1(4)$	.0659	.0602	.0544	.0489	.0430	.0372	.0516	±.0107
$P_1(5)$	.0544	.0496	.0447	.0404	.0348	.0300	.0423	±.0091
$P_1(6)$	.0438	.0399	.0359	.0329	.0278	.0241	.0341	±.0074
$P_2(3)$	.0371	.0338	.0306	.0283	.0237	.0209	.0291	±.0061
$P_1(7)$	.0347	.0317	.0288	.0268	.0224	.0199	.0274	±.0056
$P_2(4)$	.0299	.0275	.0252	.0240	.0200	.0181	.0241	±.0045
$P_1(8)$	.0269	.0250	.0230	.0223	.0188	.0172	.0222	±.0037
$P_1(5)$	.0232	.0219	.0205	.0204	.0173	.0163	.0199	±.0027
$P_2(9)$	.0205	.0195	.0186	.0191	.0163	.0158	.0183	±.0019
$P_1(6)$	.0180	.0175	.0168	.0178	.0155	.0153	.0168	±.0012
$P_2(10)$	.0151	.0153	.0153	.0168	.0151	.0152	.0155	±.0007
$P_2(7)$	.0139	.0143	.0145	.0163	.0149	.0154	.0149	±.0009
$P_3(4)$	.0119	.0147	.0136	.0159	.0152	.0160	.0146	±.0016
$P_2(8)$	.0111	.0122	.0134	.0159	.0156	.0166	.0141	±.0022
$P_3(5)$	.0102	.0117	.0133	.0164	.0165	.0178	.0143	±.0030
$P_2(9)$	.0098	.0115	.0135	.0169	.0176	.0191	.0147	±.0037
$P_3(6)$	.0095	.0117	.0138	.0175	.0187	.0203	.0153	±.0042
$P_2(10)$	.0097	.0121	.0144	.0182	.0198	.0214	.0159	±.0046
$P_3(7)$	.0100	.0125	.0148	.0187	.0206	.0222	.0165	±.0048
$P_2(11)$	.0111	.0136	.0162	.0201	.0226	.0239	.0179	±.0051
$P_3(8)$	.0116	.0142	.0169	.0207	.0233	.0246	.0186	±.0052
$P_3(9)$	.0147	.0172	.0199	.0235	.0268	.0275	.0216	±.0052
$P_3(10)$	.0191	.0215	.0239	.0271	.0311	.0310	.0256	±.0050
$P_3(10)$	.0253	.0280	.0296	.0325	.0362	.0352	.0311	±.0042

TABLE 5.

CONTRIBUTIONS TO THE WATER VAPOR CONTINUUM ABSORPTION (km^{-1}) AT AMBIENT TEMPERATURES FOR 14.3 TORR WATER VAPOR

Laser Line	k_c curve fit values 23°C	23°C Burch Extrapolations $n_s C_s (p_s + .12p_f)$	23°C $n_s C_s^A p_s$	25°C $n_s C_s^A p_s$	Average (24°C) $n_s C_s^A p_s$	24°C Burch Extrapolations $n_s C_s (p_s + .12p_s)$	ASL Modeled k_c 24°C
$P_1(2)$	.1229	.0383	.0846	.0737	.0792	.0375	.1167
$P_1(3)$	.1098	.0360	.0738	.0618	.0678	.0353	.1031
$P_1(4)$	.0977	.0337	.0640	.0516	.0578	.0330	.0908
$P_1(5)$	.0864	.0313	.0551	.0423	.0487	.0307	.0794
$P_1(6)$	.0758	.0289	.0469	.0341	.0405	.0283	.0688
$P_2(3)$	.0690	.0272	.0418	.0291	.0355	.0266	.0621
$P_1(7)$	.0666	.0265	.0401	.0274	.0338	.0260	.0598
$P_2(4)$	.0617	.0249	.0368	.0241	.0305	.0244	.0549
$P_1(8)$	.0587	.0239	.0348	.0222	.0285	.0234	.0519
$P_2(5)$	.0548	.0226	.0322	.0199	.0261	.0221	.0482
$P_1(9)$	.0518	.0216	.0302	.0183	.0243	.0212	.0455
$P_2(6)$	.0491	.0207	.0284	.0168	.0226	.0203	.0429
$P_1(10)$	.0462	.0197	.0265	.0155	.0210	.0193	.0403
$P_2(7)$	.0447	.0190	.0257	.0149	.0203	.0186	.0389
$P_3(4)$	.0424	.0181	.0243	.0146	.0195	.0177	.0372
$P_2(8)$	.0414	.0176	.0238	.0141	.0190	.0172	.0362
$P_3(5)$	.0402	.0169	.0233	.0143	.0188	.0166	.0354
$P_2(9)$	.0394	.0162	.0232	.0147	.0190	.0159	.0349
$P_3(6)$	.0389	.0161	.0228	.0153	.0191	.0158	.0349
$P_2(10)$	.0387	.0162	.0225	.0159	.0192	.0159	.0351
$P_3(7)$	.0388	.0165	.0223	.0165	.0194	.0162	.0356
$P_2(11)$	.0394	.0172	.0222	.0179	.0201	.0169	.0370
$P_3(8)$	.0399	.0176	.0223	.0186	.0205	.0172	.0377
$P_3(9)$	.0423	.0194	.0229	.0216	.0223	.0190	.0413
$P_3(10)$	.0460	.0219	.0241	.0256	.0249	.0215	.0464
$P_3(11)$	.0513	.0246	.0267	.0311	.0289	.0241	.0530

TABLE 6.

WATER VAPOR CONTINUUM ABSORPTION COEFFICIENT (km^{-1}) PREDICTIONS AT 24°C FOR STANDARD ATMOSPHERIC PRESSURE (760 TORR) USING NEW MODEL

Laser Line	RELATIVE HUMIDITY									
	10%	20%	30%	40%	50%	60%	70%	80%	90%	100%
$P_1(2)$	.0072	.0185	.0339	.0534	.0771	.1048	.1365	.1725	.2125	.2567
$P_1(3)$	.0066	.0168	.0304	.0477	.0684	.0927	.1204	.1517	.1867	.2251
$P_1(4)$	.0061	.0152	.0272	.0424	.0605	.0817	.1059	.1331	.1634	.1968
$P_1(5)$	.0055	.0136	.0242	.0374	.0532	.0716	.0924	.1159	.1420	.1706
$P_1(6)$	.0050	.0121	.0213	.0328	.0464	.0621	.0799	.1000	.1222	.1465
$P_2(3)$	.0046	.0111	.0195	.0298	.0420	.0561	.0720	.0899	.1097	.1314
$P_1(7)$	.0045	.0108	.0189	.0288	.0405	.0540	.0693	.0865	.1055	.1263
$P_2(4)$	.0042	.0100	.0174	.0265	.0373	.0496	.0636	.0793	.0966	.1155
$P_1(8)$	.0040	.0095	.0165	.0251	.0353	.0470	.0601	.0748	.0911	.1089
$P_2(5)$	.0037	.0089	.0154	.0234	.0328	.0436	.0558	.0694	.0844	.1009
$P_1(9)$	.0036	.0085	.0147	.0222	.0310	.0412	.0526	.0654	.0795	.0950
$P_2(6)$	.0034	.0080	.0139	.0210	.0293	.0389	.0496	.0616	.0748	.0893
$P_1(10)$	.0032	.0076	.0131	.0198	.0276	.0365	.0466	.0578	.0702	.0837
$P_2(7)$	.0031	.0073	.0126	.0191	.0266	.0352	.0450	.0558	.0678	.0808
$P_3(4)$	.0030	.0070	.0121	.0182	.0254	.0337	.0430	.0534	.0648	.0774
$P_2(8)$	.0029	.0068	.0117	.0177	.0247	.0328	.0418	.0520	.0631	.0753
$P_3(5)$	.0028	.0066	.0114	.0173	.0242	.0321	.0409	.0509	.0618	.0738
$P_2(9)$	.0027	.0064	.0112	.0169	.0237	.0316	.0404	.0503	.0612	.0731
$P_3(6)$	.0027	.0064	.0111	.0169	.0237	.0316	.0404	.0503	.0612	.0732
$P_2(10)$	.0027	.0065	.0112	.0170	.0239	.0318	.0406	.0506	.0616	.0736
$P_3(7)$	.0028	.0066	.0114	.0173	.0242	.0322	.0412	.0513	.0624	.0746
$P_3(11)$	.0029	.0068	.0118	.0180	.0252	.0335	.0428	.0533	.0649	.0775
$P_3(8)$	.0029	.0070	.0121	.0183	.0257	.0341	.0435	.0543	.0661	.0790
$P_3(9)$	.0032	.0076	.0133	.0201	.0281	.0374	.0478	.0595	.0723	.0864
$P_3(10)$	.0036	.0086	.0149	.0226	.0316	.0420	.0537	.0667	.0812	.0969
$P_3(11)$	.0041	.0098	.0169	.0257	.0361	.0480	.0614	.0764	.0930	.1111

DISTRIBUTION LIST

Dr. Frank D. Eaton
Geophysical Institute
University of Alaska
Fairbanks, AK 99701

Commander
US Army Aviation Center
ATTN: ATZQ-D-MA
Fort Rucker, AL 36362

Chief, Atmospheric Sciences Div
Code ES-81
NASA
Marshall Space Flight Center,
AL 35812

Commander
US Army Missile R&D Command
ATTN: DRDMI-CGA (B. W. Fowler)
Redstone Arsenal, AL 35809

Redstone Scientific Information Center
ATTN: DRDMI-TBD
US Army Missile R&D Command
Redstone Arsenal, AL 35809

Commander
US Army Missile R&D Command
ATTN: DRDMI-TEM (R. Haraway)
Redstone Arsenal, AL 35809

Commander
US Army Missile R&D Command
ATTN: DRDMI-TRA (Dr. Essenwanger)
Redstone Arsenal, AL 35809

Commander
HQ, Fort Huachuca
ATTN: Tech Ref Div
Fort Huachuca, AZ 85613

Commander
US Army Intelligence Center & School
ATTN: ATSI-CD-MD
Fort Huachuca, AZ 85613

Commander
US Army Yuma Proving Ground
ATTN: Technical Library
Bldg 2100
Yuma, AZ 85364

Naval Weapons Center (Code 3173)
ATTN: Dr. A. Shlanta
China Lake, CA 93555

Sylvania Elec Sys Western Div
ATTN: Technical Reports Library
PO Box 205
Mountain View, CA 94040

Geophysics Officer
PMTC Code 3250
Pacific Missile Test Center
Point Mugu, CA 93042

Commander
Naval Ocean Systems Center (Code 4473)
ATTN: Technical Library
San Diego, CA 92152

Meteorologist in Charge
Kwajalein Missile Range
PO Box 67
APO San Francisco, 96555

Director
NOAA/ERL/APCL R31
RB3-Room 567
Boulder, CO 80302

Library-R-51-Tech Reports
NOAA/ERL
320 S. Broadway
Boulder, CO 80302

National Center for Atmos Research
NCAR Library
PO Box 3000
Boulder, CO 80307

B. Girardo
Bureau of Reclamation
E&R Center, Code 1220
Denver Federal Center, Bldg 67
Denver, CO 80225

National Weather Service
National Meteorological Center
W321, WWB, Room 201
ATTN: Mr. Quiroz
Washington, DC 20233

Mil Assistant for Atmos Sciences
Ofc of the Undersecretary of Defense
for Rsch & Engr/E&LS - Room 3D129
The Pentagon
Washington, DC 20301

Defense Communications Agency
Technical Library Center
Code 205
Washington, DC 20305

Director
Defense Nuclear Agency
ATTN: Technical Library
Washington, DC 20305

HQDA (DAEN-RDM/Dr. de Percin)
Washington, DC 20314

Director
Naval Research Laboratory
Code 5530
Washington, DC 20375

Commanding Officer
Naval Research Laboratory
Code 2627
Washington, DC 20375

Dr. J. M. MacCallum
Naval Research Laboratory
Code 1409
Washington, DC 20375

The Library of Congress
ATTN: Exchange & Gift Div
Washington, DC 20540
2

Head, Atmos Rsch Section
Div Atmospheric Science
National Science Foundation
1800 G. Street, NW
Washington, DC 20550

CPT Hugh Albers, Exec Sec
Interdept Committee on Atmos Science
National Science Foundation
Washington, DC 20550

Director, Systems R&D Service
Federal Aviation Administration
ATTN: ARD-54
2100 Second Street, SW
Washington, DC 20590

ADTC/DLODL
Eglin AFB, FL 32542

Naval Training Equipment Center
ATTN: Technical Library
Orlando, FL 32813

Det 11, 2WS/OI
ATTN: Maj Orondorff
Patrick AFB, FL 32925

USAFETAC/CB
Scott AFB, IL 62225

HQ, ESD/TOSI/S-22
Hanscom AFB, MA 01731

Air Force Geophysics Laboratory
ATTN: LCB (A. S. Carten, Jr.)
Hanscom AFB, MA 01731

Air Force Geophysics Laboratory
ATTN: LYD
Hanscom AFB, MA 01731

Meteorology Division
AFGL/LY
Hanscom AFB, MA 01731

US Army Liaison Office
MIT-Lincoln Lab, Library A-082
PO Box 73
Lexington, MA 02173

Director
US Army Ballistic Rsch Lab
ATTN: DRDAR-BLB (Dr. G. E. Keller)
Aberdeen Proving Ground, MD 21005

Commander
US Army Ballistic Rsch Lab
ATTN: DRDAR-BLP
Aberdeen Proving Ground, MD 21005

Director
US Army Armament R&D Command
Chemical Systems Laboratory
ATTN: DRDAR-CLJ-I
Aberdeen Proving Ground, MD 21010

Chief CB Detection & Alarms Div
Chemical Systems Laboratory
ATTN: DRDAR-CLC-CR (H. Tannenbaum)
Aberdeen Proving Ground, MD 21010

Commander
Harry Diamond Laboratories
ATTN: DELHD-CO
2800 Powder Mill Road
Adelphi, MD 20783

Commander
ERADCOM
ATTN: DRDEL-AP
2800 Powder Mill Road
Adelphi, MD 20783
2

Commander
ERADCOM
ATTN: DRDEL-CG/DRDEL-DC/DRDEL-CS
2800 Powder Mill Road
Adelphi, MD 20783

Commander
ERADCOM
ATTN: DRDEL-CT
2800 Powder Mill Road
Adelphi, MD 20783

Commander
ERADCOM
ATTN: DRDEL-EA
2800 Powder Mill Road
Adelphi, MD 20783

Commander
ERADCOM
ATTN: DRDEL-PA/DRDEL-ILS/DRDEL-E
2800 Powder Mill Road
Adelphi, MD 20783

Commander
ERADCOM
ATTN: DRDEL-PAO (S. Kimmel)
2800 Powder Mill Road
Adelphi, MD 20783

Chief
Intelligence Materiel Dev & Support Ofc
ATTN: DELEW-WL-I
Bldg 4554
Fort George G. Meade, MD 20755

Acquisitions Section, IRDB-D823
Library & Info Service Div, NOAA
6009 Executive Blvd
Rockville, MD 20852

Naval Surface Weapons Center
White Oak Library
Silver Spring, MD 20910

The Environmental Research
Institute of MI
ATTN: IRIA Library
PO Box 8618
Ann Arbor, MI 48107

Mr. William A. Main
USDA Forest Service
1407 S. Harrison Road
East Lansing, MI 48823

Dr. A. D. Belmont
Research Division
PO Box 1249
Control Data Corp
Minneapolis, MN 55440

Director
Naval Oceanography & Meteorology
NSTL Station
Bay St Louis, MS 39529

Director
US Army Engr Waterways Experiment Sta
ATTN: Library
PO Box 631
Vicksburg, MS 39180

Environmental Protection Agency
Meteorology Laboratory
Research Triangle Park, NC 27711

US Army Research Office
ATTN: DRXRO-PP
PO Box 12211
Research Triangle Park, NC 27709

Commanding Officer
US Army Armament R&D Command
ATTN: DRDAR-TSS Bldg 59
Dover, NJ 07801

Commander
HQ, US Army Avionics R&D Activity
ATTN: DAVAA-O
Fort Monmouth, NJ 07703

Commander/Director
US Army Combat Surveillance & Target
Acquisition Laboratory
ATTN: DELCS-D
Fort Monmouth, NJ 07703

Commander
US Army Electronics R&D Command
ATTN: DELCS-S
Fort Monmouth, NJ 07703

Commander
US Army Electronics R&D Command
ATTN: DELCS-S (Dr. Swingle)
Fort Monmouth, NJ 07703
3

Director
US Army Electronics Technology &
Devices Laboratory
ATTN: DELET-D
Fort Monmouth, NJ 07703

Commander
US Army Electronic Warfare Laboratory
ATTN: DELEW-D
Fort Monmouth, NJ 07703

Commander
US Army Night Vision &
Electro-Optics Laboratory
ATTN: DELNV-L (Dr. Rudolf Buser)
Fort Monmouth, NJ 07703

Commander
ERADCOM Technical Support Activity
ATTN: DELSD-L
Fort Monmouth, NJ 07703

Project Manager, FIREFINDER
ATTN: DRCPM-FF
Fort Monmouth, NJ 07703

Project Manager, REMBASS
ATTN: DRCPM-RBS
Fort Monmouth, NJ 07703

Commander
US Army Satellite Comm Agency
ATTN: DRCPM-SC-3
Fort Monmouth, NJ 07703

Commander
ERADCOM Scientific Advisor
ATTN: DRDEL-SA
Fort Monmouth, NJ 07703

6585 TG/WE
Holloman AFB, NM 88330

AFWL/WE
Kirtland, AFB, NM 87117

AFWL/Technical Library (SUL)
Kirtland AFB, NM 87117

Commander
US Army Test & Evaluation Command
ATTN: STEWS-AD-L
White Sands Missile Range, NM 88002

Rome Air Development Center
ATTN: Documents Library
TSLD (Bette Smith)
Griffiss AFB, NY 13441

Commander
US Army Tropic Test Center
ATTN: STETC-TD (Info Center)
APO New York 09827

Commandant
US Army Field Artillery School
ATTN: ATSF-CD-R (Mr. Farmer)
Fort Sill, OK 73503

Commandant
US Army Field Artillery School
ATTN: ATSF-CF-R
Fort Sill, OK 73503

Director CFD
US Army Field Artillery School
ATTN: Met Division
Fort Sill, OK 73503

Commandant
US Army Field Artillery School
ATTN: Morris Swett Library
Fort Sill, OK 73503

Commander
US Army Dugway Proving Ground
ATTN: MT-DA-L
Dugway, UT 84022

William Peterson
Research Associates
Utah State University, UNC 48
Logan, UT 84322

Inge Dirmhirn, Professor
Utah State University, UNC 48
Logan, UT 84322

Defense Documentation Center
ATTN: DDC-TCA
Cameron Station, Bldg 5
Alexandria, VA 22314
12

Commanding Officer
US Army Foreign Sci & Tech Center
ATTN: DRXST-IS1
220 7th Street, NE
Charlottesville, VA 22901

Naval Surface Weapons Center
Code G65
Dahlgren, VA 22448

Commander
US Army Night Vision
& Electro-Optics Lab
ATTN: DELNV-D
Fort Belvoir, VA 22060

Commander and Director
US Army Engineer Topographic Lab
ETL-TD-MB
Fort Belvoir, VA 22060

Director
Applied Technology Lab
DAVDL-EU-TSD
ATTN: Technical Library
Fort Eustis, VA 23604

Department of the Air Force
OL-C, 5WW
Fort Monroe, VA 23651

Department of the Air Force
5WW/DN
Langley AFB, VA 23665

Director
Development Center MCDEC
ATTN: Firepower Division
Quantico, VA 22134

US Army Nuclear & Chemical Agency
ATTN: MONA-WE
Springfield, VA 22150

Director
US Army Signals Warfare Laboratory
ATTN: DELSW-OS (Dr. R. Burkhardt)
Vint Hill Farms Station
Warrenton, VA 22186

Commander
US Army Cold Regions Test Center
ATTN: STECR-OP-PM
APO Seattle, 98733

US Army Materiel Systems
  Analysis Activity
ATTN: DRXSY-MP
Aberdeen Proving Ground, MD 21005

ATMOSPHERIC SCIENCES RESEARCH PAPERS

1. Lindberg, J.D., "An Improvement to a Method for Measuring the Absorption Coefficient of Atmospheric Dust and other Strongly Absorbing Powders, " ECOM-5565, July 1975.
2. Avara, Elton, P., "Mesoscale Wind Shears Derived from Thermal Winds," ECOM-5566, July 1975.
3. Gomez, Richard B., and Joseph H. Pierluissi, "Incomplete Gamma Function Approximation for King's Strong-Line Transmittance Model," ECOM-5567, July 1975.
4. Bianco, A.J., and B.F. Engebos, "Ballistic Wind Weighting Functions for Tank Projectiles," ECOM-5568, August 1975.
5. Taylor, Fredrick J., Jack Smith, and Thomas H. Pries, "Crosswind Measurements through Pattern Recognition Techniques," ECOM-5569, July 1975.
6. Walters, D.L., "Crosswind Weighting Functions for Direct-Fire Projectiles," ECOM-5570, August 1975.
7. Duncan, Louis D., "An Improved Algorithm for the Iterated Minimal Information Solution for Remote Sounding of Temperature," ECOM-5571, August 1975.
8. Robbiani, Raymond L., "Tactical Field Demonstration of Mobile Weather Radar Set AN/TPS-41 at Fort Rucker, Alabama," ECOM-5572, August 1975.
9. Miers, B., G. Blackman, D. Langer, and N. Lorimier, "Analysis of SMS/GOES Film Data," ECOM-5573, September 1975.
10. Manquero, Carlos, Louis Duncan, and Rufus Bruce, "An Indication from Satellite Measurements of Atmospheric CO2 Variability," ECOM-5574, September 1975.
11. Petracca, Carmine, and James D. Lindberg, "Installation and Operation of an Atmospheric Particulate Collector," ECOM-5575, September 1975.
12. Avara, Elton P., and George Alexander, "Empirical Investigation of Three Iterative Methods for Inverting the Radiative Transfer Equation," ECOM-5576, October 1975.
13. Alexander, George D., "A Digital Data Acquisition Interface for the SMS Direct Readout Ground Station — Concept and Preliminary Design," ECOM-5577, October 1975.
14. Cantor, Israel, "Enhancement of Point Source Thermal Radiation Under Clouds in a Nonattenuating Medium," ECOM-5578, October 1975.
15. Norton, Colburn, and Glenn Hoidale, "The Diurnal Variation of Mixing Height by Month over White Sands Missile Range, N.M," ECOM-5579, November 1975.
16. Avara, Elton P., "On the Spectrum Analysis of Binary Data," ECOM-5580, November 1975.
17. Taylor, Fredrick J., Thomas H. Pries, and Chao-Huan Huang, "Optimal Wind Velocity Estimation," ECOM-5581, December 1975.
18. Avara, Elton P., "Some Effects of Autocorrelated and Cross-Correlated Noise on the Analysis of Variance, " ECOM-5582, December 1975.
19. Gillespie, Patti S., R.L. Armstrong, and Kenneth O. White, "The Spectral Characteristics and Atmospheric CO2 Absorption of the Ho^{+3} YLF Laser at 2.05μm," ECOM-5583, December 1975.
20. Novlan, David J. "An Empirical Method of Forecasting Thunderstorms for the White Sands Missile Range," ECOM-5584, February 1976.
21. Avara, Elton P., "Randomization Effects in Hypothesis Testing with Autocorrelated Noise," ECOM-5585, February 1976.
22. Watkins, Wendell R., "Improvements in Long Path Absorption Cell Measurement," ECOM-5586, March 1976.
23. Thomas, Joe, George D. Alexander, and Marvin Dubbin, "SATTEL — An Army Dedicated Meteorological Telemetry System," ECOM-5587. March 1976.
24. Kennedy, Bruce W., and Delbert Bynum, "Army User Test Program for the RDT&E-XM-75 Meteorological Rocket," ECOM-5588, April 1976.

25. Barnett, Kenneth M., "A Description of the Artillery Meteorological Comparisons at White Sands Missle Range, October 1974 - December 1974 ('PASS' - Prototype Artillery [Meteorological] Subsystem)," ECOM-5589, April 1976.
26. Miller, Walter B., "Preliminary Analysis of Fall-of-Shot From Project 'PASS'," ECOM-5590, April 1976.
27. Avara, Elton P., "Error Analysis of Minimum Information and Smith's Direct Methods for Inverting the Radiative Transfer Equation," ECOM-5591, April 1976.
28. Yee, Young P., James D. Horn, and George Alexander, "Synoptic Thermal Wind Calculations from Radiosonde Observations Over the Southwestern United States," ECOM-5592, May 1976.
29. Duncan, Louis D., and Mary Ann Seagraves, "Applications of Empirical Corrections to NOAA-4 VTPR Observations," ECOM-5593, May 1976.
30. Miers, Bruce T., and Steve Weaver, "Applications of Meterological Satellite Data to Weather Sensitive Army Operations,"ECOM-5594, May 1976.
31. Sharenow, Moses, "Redesign and Improvement of Balloon ML-566," ECOM-5595, June, 1976.
32. Hansen, Frank V., "The Depth of the Surface Boundary Layer," ECOM-5596, June 1976.
33. Pinnick, R.G., and E.B. Stenmark, "Response Calculations for a Commercial Light-Scattering Aerosol Counter," ECOM-5597, July 1976.
34. Mason, J., and G.B. Hoidale, "Visibility as an Estimator of Infrared Transmittance," ECOM-5598, July 1976.
35. Bruce, Rufus E., Louis D. Duncan, and Joseph H. Pierluissi, "Experimental Study of the Relationship Between Radiosonde Temperatures and Radiometric-Area Temperatures," ECOM-5599, August 1976.
36. Duncan, Louis D., "Stratospheric Wind Shear Computed from Satellite Thermal Sounder Measurements," ECOM-5800, September 1976.
37. Taylor, F., P. Mohan, P. Joseph and T. Pries, "An All Digital Automated Wind Measurement System," ECOM-5801, September 1976.
38. Bruce, Charles, "Development of Spectrophones for CW and Pulsed Radiation Sources," ECOM-5802, September 1976.
39. Duncan, Louis D., and Mary Ann Seagraves,"Another Method for Estimating Clear Column Radiances," ECOM-5803, October 1976.
40. Blanco, Abel J., and Larry E. Taylor, "Artillery Meteorological Analysis of Project Pass," ECOM-5804, October 1976.
41. Miller, Walter, and Bernard Engebos," A Mathematical Structure for Refinement of Sound Ranging Estimates," ECOM-5805, November, 1976.
42. Gillespie, James B., and James D. Lindberg, "A Method to Obtain Diffuse Reflectance Measurements from 1.0 to 3.0 μm Using a Cary 171 Spectrophotometer," ECOM-5806, November 1976.
43. Rubio, Roberto, and Robert O. Olsen,"A Study of the Effects of Temperature Variations on Radio Wave Absorption,"ECOM-5807, November 1976.
44. Ballard, Harold N., "Temperature Measurements in the Stratosphere from Balloon-Borne Instrument Platforms, 1968-1975," ECOM-5808, December 1976.
45. Monahan, H.H., "An Approach to the Short-Range Prediction of Early Morning Radiation Fog," ECOM-5809, January 1977.
46. Engebos, Bernard Francis, "Introduction to Multiple State Multiple Action Decision Theory and Its Relation to Mixing Structures," ECOM-5810, January 1977.
47. Low, Richard D.H.,"Effects of Cloud Particles on Remote Sensing from Space in the 10-Micrometer Infrared Region," ECOM-5811, January 1977.
48. Bonner, Robert S., and R. Newton, "Application of the AN/GVS-5 Laser Rangefinder to Cloud Base Height Measurements," ECOM-5812, February 1977.
49. Rubio, Roberto, "Lidar Detection of Subvisible Reentry Vehicle Erosive Atmospheric Material," ECOM-5813, March 1977.
50. Low, Richard D.H., and J.D. Horn, "Mesoscale Determination of Cloud-Top Height: Problems and Solutions," ECOM-5814, March 1977.

51. Duncan, Louis D., and Mary Ann Seagraves, "Evaluation of the NOAA-4 VTPR Thermal Winds for Nuclear Fallout Predictions," ECOM-5815, March 1977.
52. Randhawa, Jagir S., M. Izquierdo, Carlos McDonald and Zvi Salpeter, "Stratospheric Ozone Density as Measured by a Chemiluminescent Sensor During the Stratcom VI-A Flight," ECOM-5816, April 1977.
53. Rubio, Roberto, and Mike Izquierdo, "Measurements of Net Atmospheric Irradiance in the 0.7- to 2.8-Micrometer Infrared Region," ECOM-5817, May 1977.
54. Ballard, Harold N., Jose M. Serna, and Frank P. Hudson Consultant for Chemical Kinetics, "Calculation of Selected Atmospheric Composition Parameters for the Mid-Latitude, September Stratosphere," ECOM-5818, May 1977.
55. Mitchell, J.D., R.S. Sagar, and R.O. Olsen, "Positive Ions in the Middle Atmosphere During Sunrise Conditions," ECOM-5819, May 1977.
56. White, Kenneth O., Wendell R. Watkins, Stuart A. Schleusener, and Ronald L. Johnson, "Solid-State Laser Wavelength Identification Using a Reference Absorber," ECOM-5820, June 1977.
57. Watkins, Wendell R., and Richard G. Dixon, "Automation of Long-Path Absorption Cell Measurements," ECOM-5821, June 1977.
58. Taylor, S.E., J.M. Davis, and J.B. Mason, "Analysis of Observed Soil Skin Moisture Effects on Reflectance," ECOM-5822, June 1977.
59. Duncan, Louis D. and Mary Ann Seagraves, "Fallout Predictions Computed from Satellite Derived Winds," ECOM-5823, June 1977.
60. Snider, D.E., D.G. Murcray, F.H. Murcray, and W.J. Williams, "Investigation of High-Altitude Enhanced Infrared Backround Emissions" (U), SECRET, ECOM-5824, June 1977.
61. Dubbin, Marvin H. and Dennis Hall, "Synchronous Meteorlogical Satellite Direct Readout Ground System Digital Video Electronics," ECOM-5825, June 1977.
62. Miller, W., and B. Engebos, "A Preliminary Analysis of Two Sound Ranging Algorithms," ECOM-5826, July 1977.
63. Kennedy, Bruce W., and James K. Luers, "Ballistic Sphere Techniques for Measuring Atomspheric Parameters," ECOM-5827, July 1977.
64. Duncan, Louis D., "Zenith Angle Variation of Satellite Thermal Sounder Measurements," ECOM-5828, August 1977.
65. Hansen, Frank V., "The Critical Richardson Number," ECOM-5829, September 1977.
66. Ballard, Harold N., and Frank P. Hudson (Compilers), "Stratospheric Composition Balloon-Borne Experiment," ECOM-5830, October 1977.
67. Barr, William C., and Arnold C. Peterson, "Wind Measuring Accuracy Test of Meteorological Systems," ECOM-5831, November 1977.
68. Ethridge, G.A. and F.V. Hansen, "Atmospheric Diffusion: Similarity Theory and Empirical Derivations for Use in Boundary Layer Diffusion Problems," ECOM-5832, November 1977.
69. Low, Richard D.H., "The Internal Cloud Radiation Field and a Technique for Determining Cloud Blackness," ECOM-5833, December 1977.
70. Watkins, Wendell R., Kenneth O. White, Charles W. Bruce, Donald L. Walters, and James D. Lindberg, "Measurements Required for Prediction of High Energy Laser Transmission," ECOM-5834, December 1977.
71. Rubio, Robert, "Investigation of Abrupt Decreases in Atmospherically Backscattered Laser Energy," ECOM-5835, December 1977.
72. Monahan, H.H. and R.M. Cionco, "An Interpretative Review of Existing Capabilities for Measuring and Forecasting Selected Weather Variables (Emphasizing Remote Means)," ASL-TR-0001, January 1978.
73. Heaps, Melvin G., "The 1979 Solar Eclipse and Validation of D-Region Models," ASL-TR-0002. March 1978.

74. Jennings, S.G., and J.B. Gillespie, "M.I.E. Theory Sensitivity Studies - The Effects of Aerosol Complex Refractive Index and Size Distribution Variations on Extinction and Absorption Coefficients Part II: Analysis of the Computational Results," ASL-TR-0003, March 1978.
75. White, Kenneth O. et al, "Water Vapor Continuum Absorption in the 3.5μm to 4.0μm Region," ASL-TR-0004, March 1978.
76. Olsen, Robert O., and Bruce W. Kennedy, "ABRES Pretest Atmospheric Measurements," ASL-TR-0005, April 1978.
77. Ballard, Harold N., Jose M. Serna, and Frank P. Hudson, "Calculation of Atmospheric Composition in the High Latitude September Stratosphere," ASL-TR-0006, May 1978.
78. Watkins, Wendell R. et al, "Water Vapor Absorption Coefficients at HF Laser Wavelengths," ASL-TR-0007, May 1978.
79. Hansen, Frank V., "The Growth and Prediction of Nocturnal Inversions," ASL-TR-0008, May 1978.
80. Samuel, Christine, Charles Bruce, and Ralph Brewer, "Spectrophone Analysis of Gas Samples Obtained at Field Site," ASL-TR-0009, June 1978.
81. Pinnick, R.G. et al., "Vertical Structure in Atmospheric Fog and Haze and its Effects on IR Extinction," ASL-TR-0010, July 1978.
82. Low, Richard D.H., Louis D. Duncan, and Richard B. Gomez, "The Microphysical Basis of Fog Optical Characterization," ASL-TR-0011, August 1978.
83. Heaps, Melvin G., "The Effect of a Solar Proton Event on the Minor Neutral Constituents of the Summer Polar Mesosphere," ASL-TR-0012, August 1978.
84. Mason, James B., "Light Attenuation in Falling Snow," ASL-TR-0013, August 1978.
85. Blanco, Abel J., "Long-Range Artillery Sound Ranging: "PASS" Meteorological Application," ASL-TR-0014, September 1978.
86. Heaps, M.G., and F.E. Niles, "Modeling the Ion Chemistry of the D-Region: A case Study Based Upon the 1966 Total Solar Eclipse," ASL-TR-0015, September 1978.
87. Jennings, S.G., and R.G. Pinnick, "Effects of Particulate Complex Refractive Index and Particle Size Distribution Variations on Atmospheric Extinction and Absorption for Visible Through Middle-Infrared Wavelengths," ASL-TR-0016, September 1978.
88. Watkins, Wendell R., Kenneth O. White, Lanny R. Bower, and Brian Z. Sojka, " Pressure Dependence of the Water Vapor Continuum Absorption in the 3.5- to 4.0-Micrometer Region," ASL-TR-0017, September 1978.

☆ U.S. GOVERNMENT PRINTING OFFICE: 1978 777-093/ 21